Burial of organic carbon in Swedish fjord sediments : highlighting the importance of sediment accumulation rate in relation to fjord redox conditions

Burial of Organic Carbon in Swedish Fjord Sediments: Highlighting the Importance of Sediment Accumulation Rate in Relation to Fjord Redox Conditions

Emily G. Watts[1], Astrid Hylén[2, 3], Per O.J. Hall[3], Mats Eriksson[4], Elizabeth K. Robertson[3], William F. Kenney[5], and Thomas S. Bianchi[1]

[1]Department of Geological Sciences, University of Florida, Gainesville, USA
[2]Department of Biology, University of Antwerp, Wilrijk, Belgium
[3]Department of Marine Sciences, University of Gothenburg, Gothenburg, Sweden
[4]Department of Health, Medicine and Caring Sciences, Linkoping University, Linkoping Sweden
[5]Land Use and Environmental Change Institute, University of Florida, Gainesville, USA

Corresponding author: Emily G. Watts (emilygwatts@ufl.edu)

Key Points:

- Swedish fjords bury primarily marine-derived organic carbon under long-term oxic, seasonally hypoxic, and long-term anoxic water columns.
- Organic carbon burial in Swedish fjords is largely controlled by sediment accumulation rate which can limit oxygen exposure time.
- Marine-dominated fjords are uniquely efficient sinks of labile organic carbon.

Abstract

Fjords are net carbon sinks with high organic carbon (OC) burial rates; however, the key drivers of OC burial in these systems are not well constrained. To study the role of water column redox condition and OC composition on OC preservation in fjord sediments, we determined OC accumulation rates (OCAR), OC source, and OC degradation in three Swedish fjords with variable redox conditions (long-term oxic, seasonally hypoxic, and long-term anoxic). Average OCARs were variable between and within the fjords studied (2 to 122 g OC m^{-2} yr^{-2}), but highest rates were at the mouth for each fjord. Based on a $\delta^{13}C$ mixing model, Swedish fjords bury predominantly marine-derived OC (~83% of the total OC burial) likely because of relatively gentle slopes, low riverine discharge, and high marine inflow. Using a multi-biomarker approach (lignin, photosynthetic pigments, and total hydrolyzable amino acids) we found, terrestrially- and marine-derived OC were moderately degraded under the various redox conditions sampled, suggesting water column redox and OC source are not primary drivers of OC burial in these fjords. Rather, high sediment accumulation rates, common to fjords globally, lead to low oxygen exposure times, thus promoting efficient burial of OC regardless of its chemical composition.

Plain Language Summary

Fjords are net carbon sinks due in part to very high organic carbon burial rates. Despite being important in the regulation of earth's climate, the drivers of organic carbon burial in fjords are not well constrained. Here, we characterize the organic carbon buried in Swedish fjord sediments under different oxygen regimes (long-term oxic, seasonally hypoxic, and long-term anoxic) using bulk elemental and biomarker analyses. These fjords effectively bury organic carbon regardless of organic carbon source and water column oxygen conditions, likely because of high sediment accumulation rates. Fjords represent distinctive coastal systems with the capacity to retain reactive organic carbon, underscoring the importance of exploring these ecosystems in the context of global change.

1 Introduction

Anthropogenic activity has significantly altered the global carbon cycle by increasing greenhouse gas (GHG) concentrations in the atmosphere (IPCC, 2023). The ocean captures approximately 25% of this anthropogenic carbon, making it one of the major carbon sinks on earth (Gruber et al., 2023; Siegenthaler & Sarmiento, 1993). Fjords bury the most organic carbon (OC) per unit area of marine environments, burying 18-31 x 10^{12} g OC yr^{-1} (Cui et al., 2022; Smith et al., 2015). Such high OC burial rates makes fjords key in the regulation of Earth's climate on glacial-interglacial timescales (Cui et al., 2022; Smith et al., 2015). More specifically, temperate fjords have buried ca. 12% of the sediments deposited on the continental margin over the past 100 kyr despite comprising only 0.1% of the total shelf sediment volume (Nuwer & Keil, 2005). Temperate fjords are typically characterized by vegetated watersheds and high marine primary productivity, so high OC and sediment loads result in generally higher OC burial rates compared to other fjord types (e. g., subarctic, arctic glaciated, and arctic deglaciated; Cui, Bianchi, Savage, et al., 2016; Włodarska-Kowalczuk et al., 2019).

Sources of OC in fjord sediments can be characterized as a mixture of terrestrial (OC_{terr}), marine (OC_{mar}), and petrogenic (OC_{petro}) (Bianchi et al., 2020). Based on the source, the OC will have varying chemical composition and therefore stability in aquatic environments. For example, OC_{mar} (e.g., benthic macro-micro-algae, and phytoplankton) is composed primarily of amino acids, carbohydrates, and lipids, while OC_{terr} (e.g., soils and vascular-plant detritus), is rich in complex biopolymers such as lignin, cutins, and cellulose (Arndt et al., 2013). Consequently, OC_{terr} is generally regarded as more stable in marine systems than OC_{mar} and is preferentially buried long-term (Arndt et al., 2013; Burdige, 2005, 2007). Redox state has been suggested as another key driver of OC burial. For instance, under oxic environments fresh OC is typically degraded more quickly than stable OC; however, in anoxic conditions fresh OC is degraded slowly and stable OC only minimally (Bianchi et al., 2016; Burdige, 2007a; Cowie et al., 1995; Kristensen et al., 1995). Consequently, low oxygen and anoxic environments are expected to have greater OC preservation than oxic environments (Arndt et al., 2013; Bianchi et al., 2018; Middelburg & Levin, 2009). This explains the general pattern of OC burial efficiency decreasing with increasing oxygen exposure time (Hartnett et al., 1998). However, the role of redox on early diagenesis is a historically contentious topic and consequently the effect of oxygen on OC burial is poorly constrained (Arndt et al., 2013; Cowie & Hedges, 1992; Jessen et al., 2017; Van De

Velde et al., 2023; Vandewiele et al., 2009). High OC burial rates in fjords are, in part, attributed to high OC_{terr} loads and low oxygen bottom waters. However, recent studies conducted in temperate North Atlantic and Chilean fjords reported high OC content and burial rates in marine-dominated and well oxygenated systems (Á Norði et al., 2018; Faust & Knies, 2019; Lafon et al., 2014; Sepúlveda et al., 2011;Smeaton et al., 2021; Włodarska-Kowalczuk et al., 2019), thus questioning the universal role of these well-studied drivers on OC burial in fjords.

Chemical biomarkers are useful proxies to trace specific OC pools and the early diagenetic processing of the respective pools in coastal systems. There are numerous chemical biomarkers that can separate OC sources (e.g., sterols, n-alkanes, glycerol dialkyl glycerol tetraethers (GDGTs), fatty acids, lignin, photosynthetic pigments), however only a few can also serve as proxies for degradation state of the respective sources (Bianchi & Canuel, 2011). Lignin is one of the most abundant biopolymers on earth, is found strictly in vascular plants, and its degradation pathways and products are well studied which makes it a useful OC_{terr} proxy in aquatic systems (Hedges & Mann, 1979; Jex et al., 2014). Lignin has been used to determine OC_{terr} sources, contribution, degradation, and hydrodynamic sorting in fjord sediments (Cowie et al., 1992; Cui, Bianchi, Hutchings, et al., 2016; Cui, Bianchi, Savage, et al., 2016; Louchouarn et al., 1997; Walsh et al., 2008). Photosynthetic pigments (e.g., chlorophylls and carotenoids) and their degradation products (e.g., pheopigments, carotenoid chlorin esters (CCEs), steryl chlorin esters (SCEs)) can provide taxonomic information on algal communities and degradation state/pathways of the algal biomass (Chen et al., 2003; Goericke et al., 1999; King & Repeta, 1991). For instance, pigments have been used to reconstruct historical algal community shifts, determine changes in water column redox, track coastal eutrophication, and assess OC sources and quality in fjords (Bianchi, Engelhaupt, et al., 2002; Bourgeois et al., 2016; Krajewska et al., 2020; Reuss et al., 2005; Schüller et al., 2013; Smittenberg et al., 2004; Szymczak-Żyła et al., 2017; Włodarska-Kowalczuk et al., 2019). Amino acids, the building blocks of proteins, are ubiquitous in the biosphere. While amino acids are not source specific, they are useful to study OC degradation as they are relatively reactive (Cowie & Hedges, 1992, 1994; Dauwe & Middelburg, 1998). In particular, the amino acid degradation index along with non-protein amino acids are widely used in coastal and estuarine systems as indices of lability and degradation (Dauwe et al., 1999; Gaye et al., 2022). For example, amino acids have been used to study

changes in OC reactivity resulting from diagenetic processes in fjord water column and sediments (Alkhatib et al., 2012; Cowie et al., 1992; Haugen & Lichtentaler, 1991).

The global heterogeneity of fjords presents challenges in establishing universal drivers of biogeochemical cycles in these systems, such as redox control, dynamics of bottom water exchange, sources of OC, and sill depth, just to name a few (Cui, Bianchi, Savage, et al., 2016; Faust & Knies, 2019; Hinojosa et al., 2014; Smeaton & Austin, 2022). In this study, we utilized the close proximity (approximately 40 km) of three fjords with distinctly different redox regimes (e.g., long-term anoxic, seasonally hypoxic, and long-term oxic) to study the role of redox and OC composition on OC burial in fjord sediments. The primary objective was to determine how varying water column redox conditions and OC sources affects the degradation state and burial of sedimentary OC. Recent studies show that the drivers of OC burial are variable between fjords globally. This warrants further research on OC cycling in fjords as these systems are pivotal in the global carbon cycle as key aquatic critical zones susceptible to global change (Bianchi & Morrison, 2018).

2 Materials and Methods

2.1 Study Sites

Samples were collected from three fjords with varying redox conditions located on the west coast of Sweden (Fig. 1). The By, Gullmar, and Hake Fjords are located at 57-58˚N and the bottom waters are long- term anoxic, seasonally hypoxic, and long-term oxic, respectively (Fig. 2). The By and Hake Fjords are part of the Orust-Tjörn fjord system (Björk et al., 2000). The surrounding areas are covered by agriculture, forest, wetlands, and developed areas (Statistics Sweden, 2023). Given that deglaciation of the region occurred 22 to 9.7 cal kyr BP (Stroeven et al., 2016) and the predominance of igneous and metamorphic bedrock in SW Sweden (Sadeghi et al., 2013), we assume negligible OC_{petro} inputs into the fjords of this study (Cui, Bianchi, Jaeger, et al., 2016).

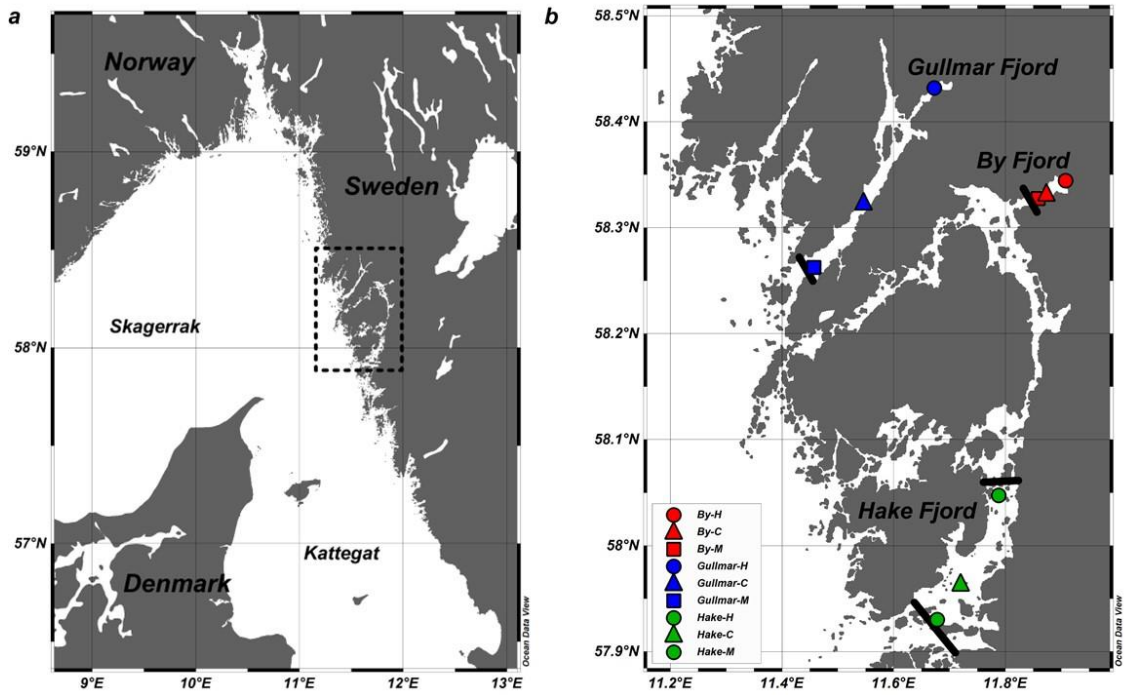

Figure 1. a) Map of sampling region outlined in the dashed box. b) The region in the dashed boxed magnified to show fjords sampled (By = red, Gullmar = blue, Hake = green) and each site within each fjord (circle = head (H), square = center (C), triangle = mouth(M)). The black lines indicate sill locations for each fjord. Map was made using Ocean Data View, (2023).

By Fjord water column is long-term anoxic below sill depth. The water column is mixed vertically every three-to-five years, but oxygen is quickly consumed resulting in oxic bottom waters for only weeks to months (Fig. 2; SMHI, 2023; Viktorsson et al., 2013). For the remainder of the three-to-five-year time period waters below the sill are anoxic and sulfidic (Viktorsson et al., 2013). By Fjord is 4 km long with a max depth of 50 m (Viktorsson et al., 2013). There is a sill located at the western-most end at 13 m depth (Viktorsson et al., 2013). The Bäve River discharges at the head of the fjord with an average rate of 4-8 m^3 s^{-1} (Stigebrandt et al., 2015; Viktorsson et al., 2013). Starting in 2010, By Fjord was the location of a 2.5 year long environmental engineering experiment in which surface waters were pumped into deep waters and resulted in the fjord becoming oxic from December 2010 to August 2013 (Stigebrandt et al., 2015). The fjord has now returned to its long-term anoxic conditions (Fig. 2; SMHI, 2023).

The bottom waters of Gullmar Fjord are seasonally hypoxic (Fig. 2; SMHI, 2023). Despite the presence of a sill, the bottom waters of Gullmar Fjord are renewed annually,

typically in late winter/spring when the thermocline is not well established (Filipsson & Nordberg, 2004; Svansson, 1984). Oxygen concentrations decrease starting in June and drop below 2 mL O_2 L^{-1} (89 µM = 2.8 mg L^{-1}) and are considered hypoxic in the deepest part of Gullmar Fjord by November-January (Fig. 2; Filipsson & Nordberg, 2004; Polovodova Asteman & Nordberg, 2013; SMHI, 2023). Oxygen levels lower than 1 mL O_2 L^{-1} (45 µM = 1.4 mg L^{-1}) can occur if deep-water exchanges do not or only partially occur (Fig. 2; Filipsson & Nordberg, 2004; Polovodova Asteman & Nordberg, 2013; SMHI, 2023). Such low values have been recorded on multiple occasions and are becoming more frequent (Filipsson & Nordberg, 2004). Gullmar Fjord is 28 km long and approximately 119 m deep (McQuoid & Nordberg, 2003). The sill depth is approximately 50 m. The Örekil river drains into the head of the fjord with an average discharge of 24 m^3s^{-1} (Brinkmann et al., 2022).

Hake Fjord is the southernmost fjord of the Orust-Tjörn system (Björk et al., 2002) with a water column characterized as long-term oxic (Fig. 2; SMHI, 2023). It is 22 km long, 5 km wide, and is connected to Havstensfjord at the north end and to the Skagerrak at the south end (Björk et al., 2002). The maximum depth in this fjord is approximately 65 m. There is a sill at the south end at 25 m and at 20 m at the north end (Björk et al., 2002). This fjord is understudied compared to By and Gullmar Fjords.

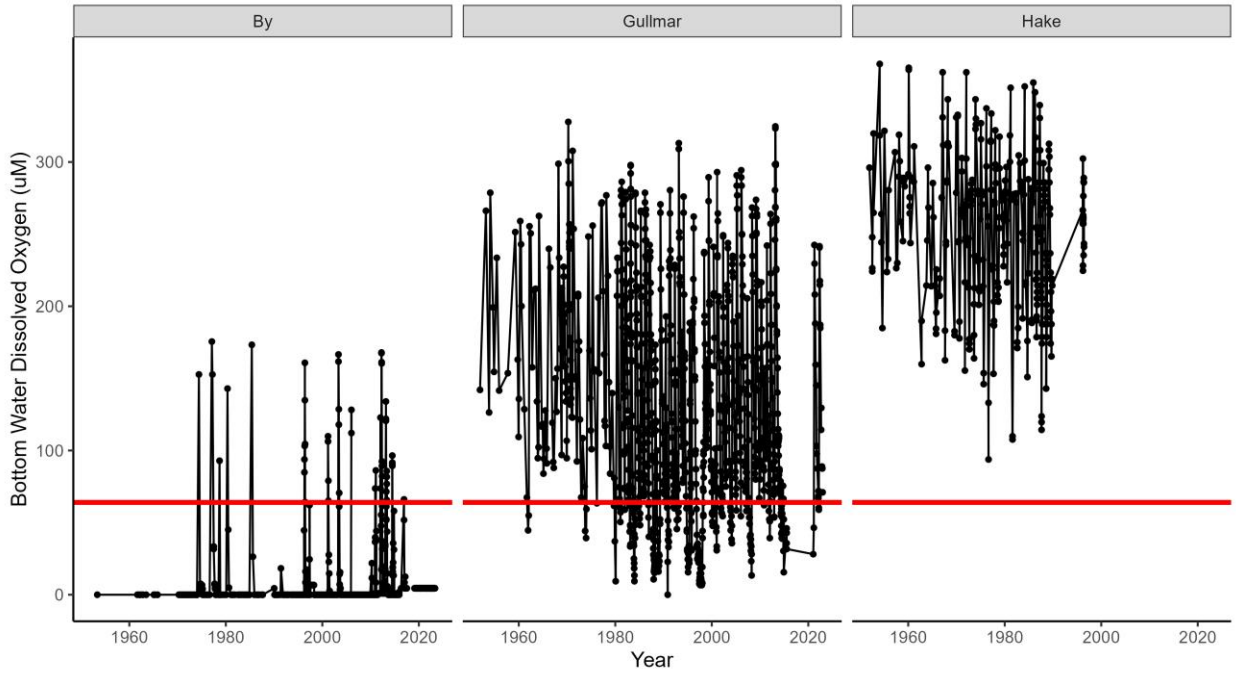

Fig. 2. Bottom water dissolved oxygen concentrations (µM) for the By (water depth ≥ 40 m), Gullmar (water depth ≥ 110 m), and Hake Fjords (water depth ≥ 20 m) from 1951 to 2023. The red line indicates 64 µM. Dissolved oxygen data is from SMHI, (2023).

2.2 Sample Collection

Sediment cores were collected from nine locations within the three fjords aboard the R/V *Skagerrak* in September-October 2021. These cores were collected from the head, center, and mouth stations (H, C, and M, respectively) of the By, Gullmar, and Hake Fjords (Table 1, Fig. 1b). Prior to sediment sampling, a CTD cast was made at each station to measure water column salinity, water column dissolved oxygen, temperature, and water depth. Approximately 20 cm long sediment cores were collected using a GEMAX sediment corer (9 cm inner diameter). One core was collected for radionuclide determinations, a second core was collected for elemental, lignin, and total hydolyzable amino acid analysis, and a third core was collected for grain size and sediment surface area analysis. These cores were sliced at 1 cm intervals, from 0 cm to 6 cm and at 2 cm intervals from 6 cm to 20 cm, placed in Whirlpak bags, and immediately frozen at -20˚C. Sediment samples for pigment analysis were sub-sampled from a fourth core that was sliced at 0.5 cm intervals to 2 cm, 1 cm intervals to 6 cm, and 2 cm intervals to the bottom of the core. Pigment samples were placed in 15 mL falcon tubes and immediately stored in liquid nitrogen. Marine end-member samples were collected using a 20 µm mesh plankton tow outside the mouth station of Gullmar Fjord. Terrestrial end-member samples, which included vascular plants and soils, were collected from the watershed shorelines of Gullmar and By Fjords and were immediately frozen. Sediment and end-member samples remained frozen until arrival at the University of Gothenburg, Sweden. Sediment samples (except those collected for pigment analysis) were freeze-dried, transferred to pre-combusted square 60 mL glass bottles, and homogenized on a roller-mill (Arnold & Schepers, 2004).

2.3 Elemental Analysis and Bulk Sediment Characterization

Bulk sediment samples were analyzed for OC, total nitrogen (TN), and the stable isotopes of carbon ($\delta^{13}C$) and nitrogen ($\delta^{15}N$). Inorganic carbon was removed from samples by acid fumigation with 12 N HCl and subsequent drying at 60˚C (Harris et al., 2001). Total organic carbon (TOC), TN, and $\delta^{13}C$ were measured on a Carlo Erba NA1500 CNS elemental analyzer

208 coupled to a Thermo Electron DeltaV Advantage isotope ratio mass spectrometer (IRMS) at the
209 Stable Isotope Mass Spectrometry Laboratory, Department of Geological Sciences, University of
210 Florida. The standard deviation of replicate standards (USGS40; n = 55) was 0.3% and 0.09% for
211 %OC and $\delta^{13}C$, respectively. Both OC and TN are expressed as percent of dry sediment mass,
212 %OC and %TN, respectively, and stable isotope data is reported in $\delta^{13}C$ (‰) notation relative to
213 the Vienna Pee Dee Belemnite standard. The molar ratio of organic carbon to nitrogen (C/N) was
214 calculated as (%OC/12)/(%TN/14).

215 The relative contribution of OC_{terr} and OC_{mar} in sediments was calculated using a
216 Bayesian isotopic-mixing model with the MixSIAR package in RStudio (Stock et al., 2018). The
217 measured terrestrial end-member $\delta^{13}C$ input value used was -29.4 ± 0.8‰ (n = 16). The measured
218 marine end-member $\delta^{13}C$ value was -18.9‰ (n=1). Additional phytoplankton isotope data for the
219 marine end-member value were taken from Olofsson et al. (2019) and Waite et al. (2005).The
220 marine end-member input value used in the model was -20.1 ± 1.6‰ (n=19). The Markov Chain
221 Monte Carlo model was run with uninformative priors, 1,000,000 chain length, 500,000 burn-in
222 iterations, a thinning factor of 500, and three chains (Stock et al., 2018). The mean and standard
223 deviation of the posterior distribution of OC source were calculated for each sample.

224 Percent mud, or the percent sediment grain-size <63 µm, was determined for surface
225 sediments (0 to 1 cm) for each site via wet sieving. Organic matter was removed from sediment
226 samples using H_2O_2, and samples were wet sieved using Calgon through a 63 µm mesh size
227 sieve. Percentages were determined by mass. Sediment surface area and pore volume was
228 determined for surface sediments (0 to 1 cm) for each site by N_2 gas adsorption and BET data
229 evaluation for pores >1.5 nm according to the theory described by Kwon & Pignatello, (2005) on
230 a Quantachrome Autosorb I at the Particle Engineering Research Center, University of Florida.

231 ### 2.4 ^{210}Pb, Mass Accumulation Rates, and Organic Carbon Accumulation Rates

232 The determination of ^{210}Pb activity was done through its progeny ^{210}Po assumed to be in
233 secular equilibrium. Polonium analysis require radiochemical separation and measurements in
234 alpha spectrometer. We used a slightly modified Po separation method earlier described by Flynn
235 (1968), Ehinger et al. (1986), and Henricsson et al. (2011). See supplementary information (Text
236 S1) for more details. The support level of ^{210}Pb, assumed to be in secular equilibrium with ^{226}Ra,
237 was calculated as the average activity of ^{226}Ra daughters (^{214}Pb and ^{214}Bi) in some selected

sediment slices of each core. The samples were sealed in radon-tight containers and left for three weeks to ensure the equilibrium between ^{226}Ra and its progenies and to prevent radon leakage (Mauring & Gäfvert, 2013). The sealed samples were measured for 2 to 3 days on a high-purity germanium detector (HPGe).

The sediment mass accumulation rate (MAR) for each site was calculated using a ^{210}Pb-dating method assuming constant flux and constant sedimentation (CFCS) of ^{210}Pb to the sediments (Appleby & Oldfield, 1978). For CFCS modelling a non-linear fitting (NLS) function was used where the measured total ^{210}Pb data was fitted to gain the MAR results (Törnquist et al., 2023). To evaluate the MAR uncertainties a Monte Carlo procedure was used simulating about 1000 data sets for the CFCS modelling (Törnquist et al., 2023).

Average OC content and OC accumulation rates (OCAR) for each site were calculated using the following equations:

$$OC_{site} = \sum_i^n (OC_i \times dry\ mass_i) \Big/ \sum_i^n (dry\ mass_i)$$

$$OCAR_{site} = OC_{site} \times MAR_{site}$$

where, OC_i and dry $mass_i$ are the OC content and dry mass of slice *i* within each core at each site. OC_{site} and $OCAR_{site}$ are the average OC content and OCAR for each site, respectively. Core slices 10 cm and deeper were used to calculate OC_{site} as By-H exhibited decreasing OC content with depth. Average OC content and OCAR for each fjord and the region of SW Sweden was calculated following the approach of Cui, Bianchi, Savage, et al. (2016).

2.5 Amino Acids

Total hydrolyzable amino acids (THAA) were determined by hydrolyzing sediment equivalent to 3 ± 0.5 mg OC dried sediment with 1.0 mL 6 N hydrochloric acid (HCl) at 110˚C for 20 hours under N_2 atmosphere (Shields, Bianchi, Osburn, et al., 2019). The THAA pool was analyzed using the Thermo Fisher Ultimate 3000 UPLC coupled to the FLD-3100 Fluorescence Detector (excitation at 330 nm and emission at 418 nm) following the pre-column o-phthaldialdehyde (OPA) derivatization technique, as described by (Lindroth & Mopper, 1979). Individual amino acids were separated using a C_{18} reverse-phase column (Adsorbosphere C18; 250 mm x 4.6 mm x 5 µm) following the method described in Shields, Bianchi, Osburn, et al.

(2019). Individual amino acids were quantified from a 5-point calibration curve of standards of each amino acid quantified (Pierce Standard-H). Pierce Standard-H did not include the non-protein amino acids β-alanine or γ-aminobutyric acid, so these were individually added to the mixture.

The amino acid degradation index (DI) is based on changes in mol % of amino acids (excluding non-protein amino acids) and can be used to quantify the degradation of the organic matter in sediments (Dauwe et al., 1999). The DI score is calculated with the following equation:

$$DI = \sum_i [\frac{var_i - AVG\ var_i}{SD\ var_i}] \times fac.coef._i$$

where, Var_i is the mol % from the sample, AVG var_i is the mean, SD var_i is the standard deviation, and $fac.coef._i$ is the loadings/scoring on the first principle component from Dauwe et al. (1999). The DI values are useful in separating differences between fresh (DI > 0.5), intermediately degraded (0.5 > DI > -0.5), and severely degraded (DI<-0.5) material (Dauwe et al., 1999). During our analysis, we had issues detecting histidine (His), but excluding His has been found to not significantly impact DI calculations (Vandewiele et al., 2009). Other THAA degradation parameters include %N-THAA, where higher values correlate to fresher material, and mol% non-protein amino acids (e.g. β-alanine (BALA)), where higher percentages correspond to more degraded material.

The Ox/Anox index is based on the reactivities of individual amino acids under oxic and anoxic conditions and is calculated with the following equation using molar % of each compound:

$$\frac{Ox}{Anox} = \frac{Asp + Glu + BALA + GABA + Lys}{Ser + Met + Ile + Leu + Tyr + Phe}$$

where, Ox/Anox ratios ≥ 1.5 are indicative of degradation under oxic conditions and Ox/Anox ratios ≤ 1 are indicative of degradation under anoxic conditions (Menzel et al., 2013, 2015). While this ratio was initially applied to study redox in lacustrine systems, it has been used in numerous coastal studies (Gaye et al., 2022; Mai-Thi et al., 2017).

287 2.6 Lignin

288 Lignin phenols were extracted following the cupric oxide oxidation (CuO) method
289 (Hedges & Ertel, 1982), as modified by Goñi & Hedges, (1995). The lignin oxidation products
290 (LOPs) were separated with an Aligent DB-5ms column (30 m length, 0.25 mm ID) on a Thermo
291 Scientific Trace 1310 Gas Chromatogram coupled to a Thermo Scientific TSQ8000 Triple
292 Quadrupole Mass Spectrometer as outlined in (Shields, Bianchi, Kolker, et al., 2019). All
293 calculations were done using relative response factors where peak areas were normalized to the
294 instrument standard (methyl 3,4-dimethoxy benzoate) to account for instrument variability.
295 Individual lignin phenols were quantified from a log-transformed 7-point calibration curve. A
296 standard mixture was made from solid compounds purchased from Sigma Aldrich and Acros
297 Organics.

298 The eight major LOPs can be subdivided into vanillyl (V), syringyl (S), and cinnamyl (C)
299 phenols (Hedges & Ertel, 1982). The sum of total V, S, and C phenols normalized to 100 mg OC
300 is represented as Λ_8 and is a proxy for OC_{terr} inputs. Ratios of C/V and S/V phenols can indicate
301 woody versus non-woody and angiosperm versus gymnosperm sources, respectively (Hedges &
302 Mann, 1979). Additional LOPs quantified include p-hydroxy (P) phenols and 3,5-
303 dibhydroxybenzoic acid (3,5-Bd). The ratio of 3,5-Bd/V is a proxy for soil inputs (Otto &
304 Simpson, 2006). P/S+V and $(acid/aldehyde)_v$ ($(Ad/Al)_v$) ratios are indicative of lignin
305 decomposition where higher values (>0.3) indicate greater extent of degradation (Hedges,
306 Blanchette, et al., 1988; Jex et al., 2014; Opsahl & Benner, 1995).

307 2.7 Plant Pigments

308 For pigment analysis, 1 gram of wet sediment was extracted with 10 mL 20:80 methanol:
309 acetone for 24 hours at -20 ˚C. Samples were sonicated for 1 min. and syringe filtered with a
310 0.45 µm nylon filter. Pigment extracts were analyzed by high performance liquid
311 chromatography (HPLC; Shimadzu UV/VIS Photodiode array detector SPD-M20A) with a C18
312 column (Shim-pack GIST C18; 3 µm; 150 x 4.6 mm) according to the method described by
313 Wright and Jeffrey (1997). Pigments concentrations were determined from a 4-point calibration
314 curve. Chlorophyll-a, fucoxanthin, zeaxanthin, pheophorbide-a and pheophytin-a standards were
315 purchased from DHI LAB. Chlorophyll-a was quantified at 436 nm, carotenoids were quantified
316 at 450 nm, and pheopigments were quantified at 410 nm. Pheopigments here include pheophytin-

a, pheophytin-a-like, and pheophorbide-a-like pigments. Pheophorbide-a was not quantified because of co-elution with other pigments.

Chlorophyll-a is a pigment found in all photosynthetic organisms which makes it a useful proxy for total algal biomass (Roy et al., 2011). Pheophytin-a and pheophorbide-a are degradation products of chlorophyll-a, and the ratio of chlorophyll-a/pheopigments can be used to quantify degradation state (Roy et al., 2011). Fucoxanthin and zeaxanthin are both carotenoids found in numerous organisms, but are major pigments in diatoms and cyanobacteria, respectively (Roy et al., 2011).

2.8 Statistical Analysis

Prior to statistical analysis, linear assumptions were checked using the Shapiro-Wilk test ($p > 0.01$) and Levene test ($p > 0.05$). To compare measured parameters between sites, a one-way ANOVA with Tukey's test for multiple comparisons was conducted. If the assumption of normality was met but the data was heteroscedastic, Welch's ANOVA was used. A p-value<0.05 was the threshold for significance. All data handling was conducted in Excel and R-Studio.

3 Results

3.1 Total Organic Carbon, Total Nitrogen, Stable Carbon Isotopes, and Sediment Characterization

The %OC in By-H sediments decreased downcore from 2.4% in surface sediments to an average of 0.5 ± 0.1% at 9-20 cm (Fig. 3a, Table S1). Conversely, %OC in sediment samples for all other stations showed minimal change with depth and ranged from 2.2 to 2.7% (Fig. 3a, Table S1). Molar C/N ratios at all sites ranged from 8.8 to 14.6 and were significantly higher at sites adjacent to rivers, sites By-H (0-5 cm) and Gullmar-H, compared to all other sites (Table S1, Fig. S2a). Similarly, $\delta^{13}C$ values ranged from -26.2% to -21.4% with significantly lowest values at Gullmar-H and By-H surface sediments (0-5 cm; Fig. 3b, Table S1). $\delta^{15}N$ values did not change with depth and ranged from 6‰ to 7‰, except for at By-H (0-5 cm) and Gullmar-H, where values were somewhat lower (Table S1, Fig. S2b).

The highest average OC_{mar} contributions were found in Hake Fjord, ranging from 78% to 90% OC_{mar} (Fig 3c, Table S1). Gullmar and By Fjords had a wider range of OC_{mar} contributions,

ranging from 30% to 79% and 38% to 76%, respectively (Table S1), with lowest contributions at the head stations (Fig. 3c).

Mud content (% <63 µm) ranged from 91.2% to 95.4% in By Ford, 87.7% to 93.1% in Gullmar Fjord and 92.5% to 95.4% in Hake Fjord (Table 1). Organic carbon: surface area ratios (OC:SA) ranged from 1.1 to 2.7 in By Fjord, 0.9 to 1.8 in Gullmar Fjord and 1.1 to 1.2 in Hake Fjord (Table 1).

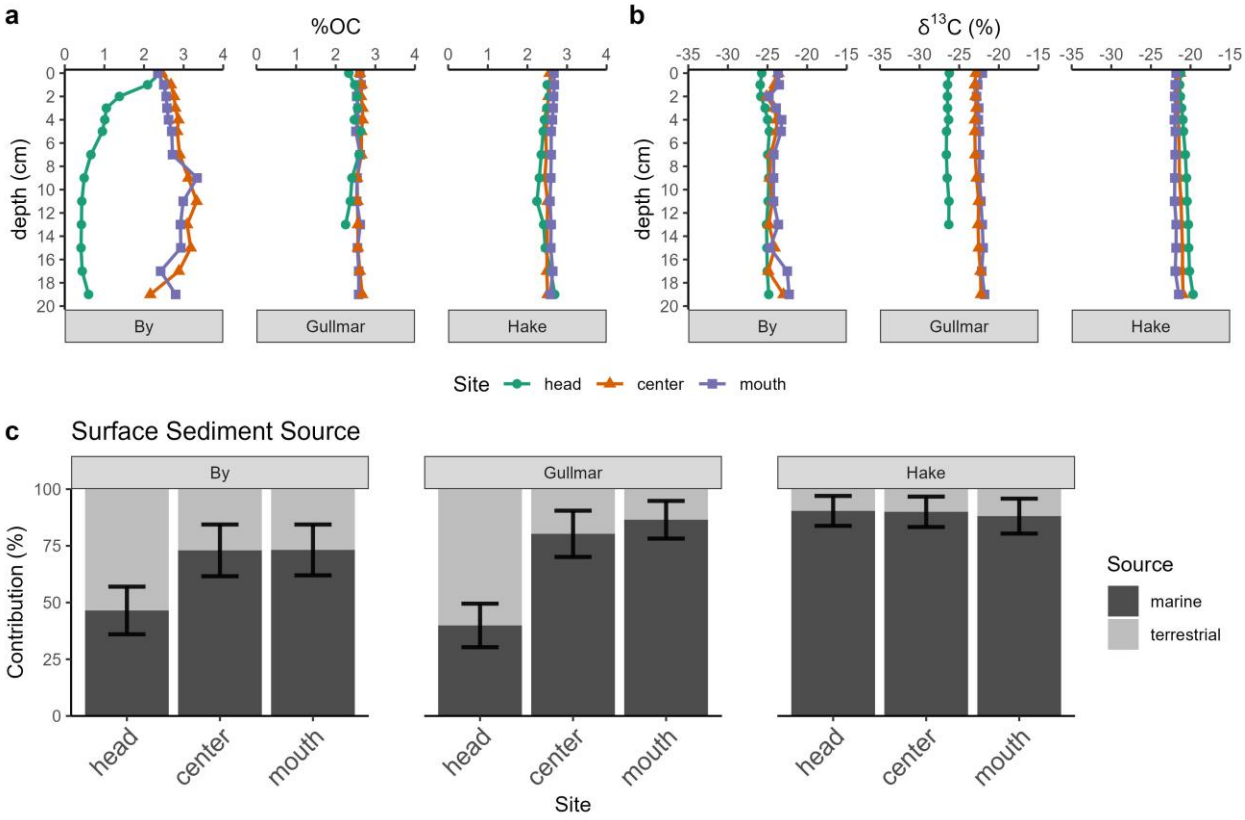

Figure 3. Downcore profiles of a) organic carbon content (%OC) and b) $\delta^{13}C$ values (%) faceted by fjord and colored by site id. c) Surface sediment source (1 cm) from the MCMC mixing model where the gray error bars represent 1 SD.

Table 1. *Sampling Site Information.* Site ID, water depth, bottom water dissolved oxygen (DO) at time of sampling, long-term redox conditions, surface mixed layer (SML) depth, surface mud content (<63 µm), sediment mass accumulation rate (MAR), organic carbon accumulation rate (OCAR) and marine organic carbon accumulation rate ($OC_{mar}AR$) are displayed. Averages for each fjord are reported where possible. * SML depth at By-C and By-M is assumed to be 0, and the apparent SML depth is likely an artefact of sampling.

Fjord, Station	Site ID	Water depth (m)	Bottom water DO (µM)	Long-term redox	SML depth (cm)	Surface mud content (<63 µm)	Surface OC:SA (mg OC m^{-2})	MAR (g m^{-2} yr^{-1})	OCAR (g m^{-2} yr^{-1})	$OC_{mar}AR$ (g m^{-2} yr^{-1})
By, Head	By-H	11	260	Oxic	0	91.6	1.1	470 ± 40	2 ± 1	1± 0.1
By, Center	By-C	46.5	0	Anoxic	0*	91.2	2.7	380 ± 10	12 ± 3	8 ± 2
By, Mouth	By-M	23	0	Anoxic	0*	95.4	2.4	840 ± 90	24 ± 3	18 ± 2
By AVG								**560 ± 50**	**13 ± 5**	**9 ± 4**
Gullmar, Head	Gullmar-H	26	175	Oxic	10	87.7	1.8	670 ± 80	16 ± 2	6 ± 1
Gullmar, Center	Gullmar-C	118	107	Seasonally Hypoxic	12	92.0	0.9	1500 ± 200	39 ± 5	32 ± 6
Gullmar, Mouth	Gullmar-M	57	164	Seasonally Hypoxic	4	93.1	1.4	2220 ± 220	57 ± 6	49 ± 5
Gullmar AVG								**1460 ± 100**	**38 ± 12**	**29 ± 10**
Hake, Head	Hake-H	21	213	Oxic	0	93.4	1.1	1150 ± 80	28 ± 2	26 ± 2
Hake, Center	Hake-C	32	199	Oxic	3	92.5	1.1	1640 ± 110	41 ± 3	37 ± 3
Hake, Mouth	Hake-M	41	204	Oxic	4	95.4	1.2	4700 ± 500	122 ± 14	107 ± 12
Hake AVG								**2500 ± 170**	**64 ± 20**	**56 ± 18**

Total AVG	**1500 ± 70**	**38 ± 24**	**31 ± 21**

363 3.2 Surface Mixed Layers, Mass Accumulation Rates and OC Accumulation Rates

364 Excess ^{210}Pb profiles showed clear evidence of a surface mixed layer (SML) at most sites
365 (Fig. S1). SML depths ranged from 0 to 12 cm (Table 1). Despite being long-term anoxic, By-C
366 and By-M had evidence of SMLs. However, no macrobenthic organisms were found in the
367 sediment cores during coring or slicing (pers. obs.), so the SML cannot be from bioturbation.
368 The apparent SML in this fjord may have been an artifact of coring disturbance due to the
369 presence of a significant flocculent layer in the surface sediments of By Fjord anoxic basin.

370 Average mass accumulation rates (MARs) and organic carbon accumulation rates
371 (OCARs) increased moving from the head to the mouth of each fjord (Table 1, Fig. 4). Highest
372 MARs and OCARs were found in Hake Fjord with average MAR ranging from 1150 ± 80 g m^{-2}
373 yr^{-1} to 4700 ± 500 g m^{-2} yr^{-1} and OCARs ranged from 28 ± 2 g OC m^{-2} yr^{-1} to 122 ± 14 g OC m^{-2}
374 yr^{-1} (Table 1, Fig. 4). Lowest MARs and OCARs were found in By Fjord with average MAR and
375 OCAR values ranged from 380 ± 10 g m^{-2} yr^{-1} to 840 ± 90 g m^{-2} yr^{-1}, and 2 ± 1 g OC m^{-2} yr^{-1} to
376 24 ± 3 g OC m^{-2} yr^{-1}, respectively (Table 1, Fig. 4).
377

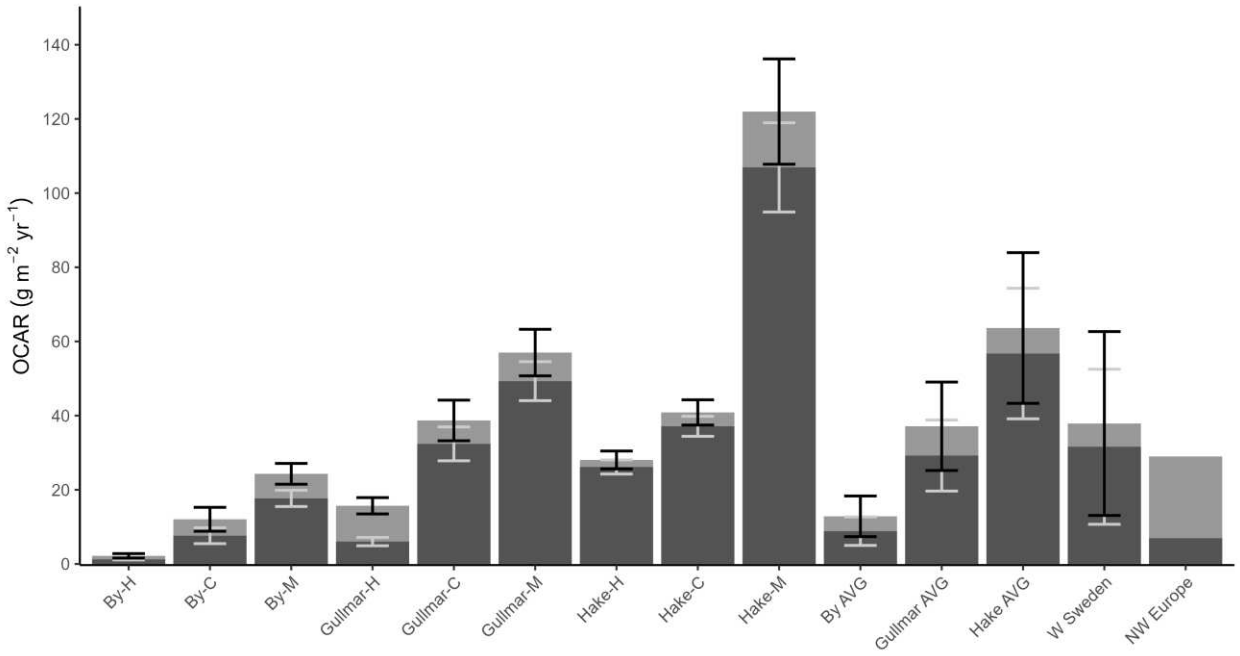

378
379 **Figure 4.** Organic carbon accumulation rates (OCAR) for each site and the darker shaded areas
380 represent marine organic carbon accumulation rates ($OC_{mar}AR$). Averages for each fjord and

overall are indicated by AVG. Error bars represent 1SD. Values for NW Europe are from Cui et al., (2016).

3.3 Total Hydrolyzable Amino Acids

At some sites (e.g. By-H, By-C, By-M, and Hake-H), THAA concentrations were highest in the top 0-2 cm of sediments, ranging from 1.1 to 3.7 mmol gC^{-1}, but decreased to 2 cm and stabilized below that depth (Fig. 5a). For inter-site comparison, averages are based on 2-20 cm concentrations of all cores. The THAA concentrations were significantly lower at By-H (2.1 ± 0.6 mmol gC^{-1}) and Hake-H (4.1 ± 0.5 mmol gC^{-1}) compared to all other sites (Table S1, Fig. 6a). Average %N-THAA is very similar between long-term anoxic sites (By-H, -C), seasonally hypoxic sites (Gullmar-C, -M), and long-term oxic sites (Hake-C, -M),with averages ranging from 19% to 43% (Table S1, Fig. S3a).

Average DI values for all sites fell between -0.5 and 0.5 (Table S1, Fig. 6b), however Gullmar-C had significantly lower DI values than all stations besides Gullmar-M (Table S1; Fig. 5b). There were no clear trends of Ox/Anox ratios as they were not statistically different between long-term anoxic sites By-C and By-M, seasonally hypoxic site Gullmar-M, and long-term oxic sites Hake-H, Hake-C, and Hake-M (Fig. S3b). All sites had average ratios < 1.5, excluding By-H (1.5 ± 0.2) and Gullmar-C (1.6 ± 0.1; Fig. S3b, Table S1).

Mol % BALA increased with depth at By-H and therefore do not meet assumptions for statistical testing, so values are reported as ranges. Mol % BALA was highest at By-H which range from 1.1 to 8.4%. Gullmar-C also had high mol % BALA with values ranging from 0.4 to 5.4% (Fig. S3c, Fig. S4). Values at all other sites (By-C, By-M, Gullmar-H, Gullmar-M, Hake-H, Hake-C, and Hake-M), including long-term anoxic, seasonally hypoxic, and long-term oxic, were 0.4 to 3.8% (Fig. S3c, Fig. S4).

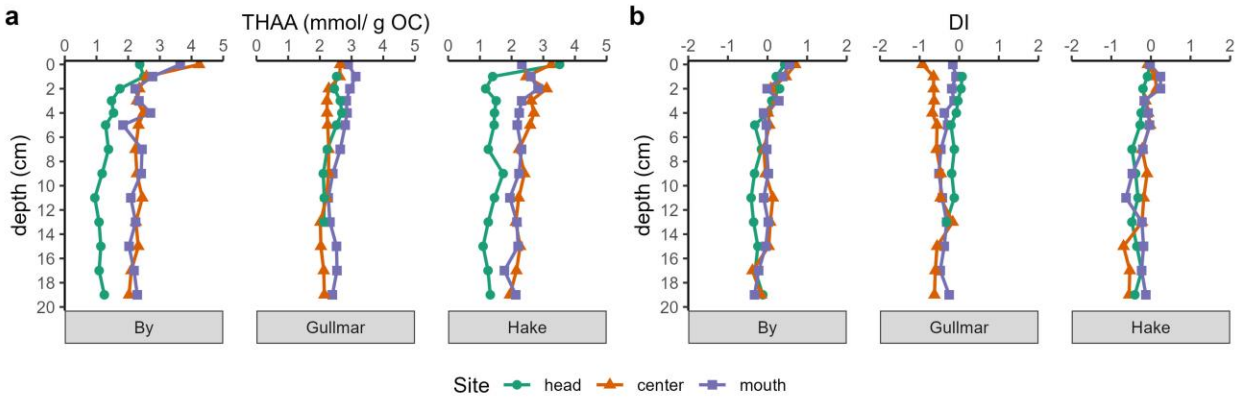

Figure 5. Downcore profiles of a) total hydrolyzable amino acid (THAA) concentrations and b) degradation index (DI) values. Each subfigure is faceted by fjord id and color coded by site id.

3.4 Lignin Oxidation Products

Values of Λ_8 decreased at By-H, which coincides with decreases in OC content. Therefore, only the top 0 to 5 cm were used from By-H for inter-site comparison of OC_{terr} inputs. Values of Λ_8 were significantly highest at Gullmar-H (2.7 ± 0.1 mg (100 mg OC)$^{-1}$) and By-H (2.0 ± 0.3 mg (100 mg OC)$^{-1}$), both of which are adjacent to rivers (Fig. 5, Table S1). More distal sites in By Fjord (By-C, -M), had significantly higher Λ_8 values (1.3 ± 0.2 mg (100 mg OC)$^{-1}$) than those in Gullmar Fjord and all sites in Hake Fjord (Hake-H, -C, and -M) with average Λ_8 values ranging from 0.6 to 0.9 mg (100 mg OC)$^{-1}$ (fig. 5, Table S1) .

Ratios of S/V and C/V change with depth and therefore do not meet assumptions for statistical testing. Therefore, values are reported as ranges. C/V and S/V ratios ranged from 0.19 to 0.67 and 0.48 to 0.98, respectively (Fig. 5c, Table S1, Fig.S5a-b). Both C/V and S/V ratios were lower at sites next to rivers including By-H and Gullmar-H compared to all other sites (Fig. 5c, Table S1, Fig.S5a-b). Ratio of 3,5-Bd/V also change with depth, so ranges are reported. Ratios of 3,5-Bd/V were lowest at By-H (0.07 to 0.2) and Gullmar-H (0.06 to 0.08) and were similar at all other sites ranging from 0.08 to 0.26 (Fig. S5d).

Ratios of $(Ad/Al)_v$ were significantly lowest at head stations adjacent to rivers, By-H (0.39 ± 0.05) and Gullmar-H (0.26 ± 0.02), compared to other stations within the same fjord (Fig. 6b, Table S1). There were no clear differences at all other sites with $(Ad/Al)_v$ averages ranging from 0.41 ± 0.08 to 0.53 ± 0.05 (Fig. 6b, Table S1). P/S+V ratios were significantly

lowest at By-H (0.18 ± 0.03) and Gullmar-H (0.12 ± 0.004) and highest at Gullmar-M (0.40 ± 0.04; Fig. S5c, Table S1). There were no significant differences at all other sites with averages ranging from 0.26 ± 0.03 to 0.29 ± 0.01 (Fig. S5c, Table S1).

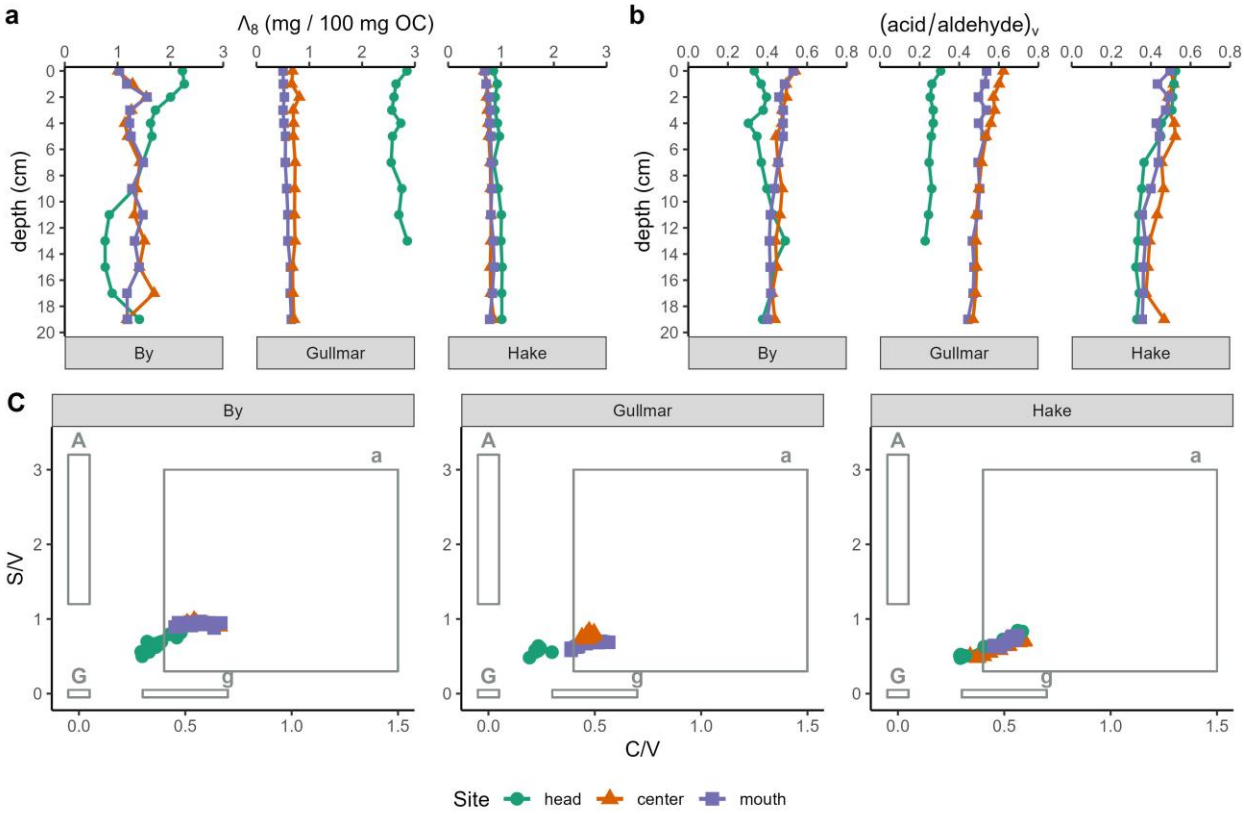

Figure 6. Downcore profiles of a) Λ_8, a measure of total lignin concentration and b) $(acid/aldehyde)_v$ ratios, a lignin degradation parameter. c) Plot of syringyl to vanillyl (S/V) versus cinnamyl to vanillyl (C/V) ratios and typical values of woody angiosperms (A), nonwoody angiosperms (a), woody gymnosperms (G), and nonwoody gymnosperms (g) in gray. Each subfigure is faceted by fjord and color coded by site.

3.5 Plant Pigments

Chlorophyll-a and fucoxanthin concentrations decreased sharply with depth in sediments at all sites but were much higher at By-C and By-M (315 to 4367 nmol gOC^{-1} and 68 to 1357 nmol gOC^{-1}, respectively) than at all other sites (below limit of detection (BLD) to 1801 nmol gOC^{-1} and BLD to 834 nmol gOC^{-1}, respectively; Fig. 7a-b). Zeaxanthin concentrations did not have any clear downcore trends and were higher at By-M and By-C (82 to 1118 nmol gOC^{-1}) than at all other sites (BLD to 416 nmol gOC^{-1}; Fig. 7c). Pheopigment concentrations were

higher and relatively stable at By-C and By-M (1242 to 4469 nmol gOC^{-1}) compared to all other sites where concentrations sharply decreased with depth (115 to 2093 gOC^{-1}; Fig. 7d) Chlorophyll to pheopigment ratios (Chl-a/pheo) were highest in By Fjord surface sediments with ratios ranging from BLD to 1.38. in Gullmar and Hake Fjords, Chl-a/pheo ratios ranging from 0.13 to 0.61 and 0.08 to 0.49, respectively.

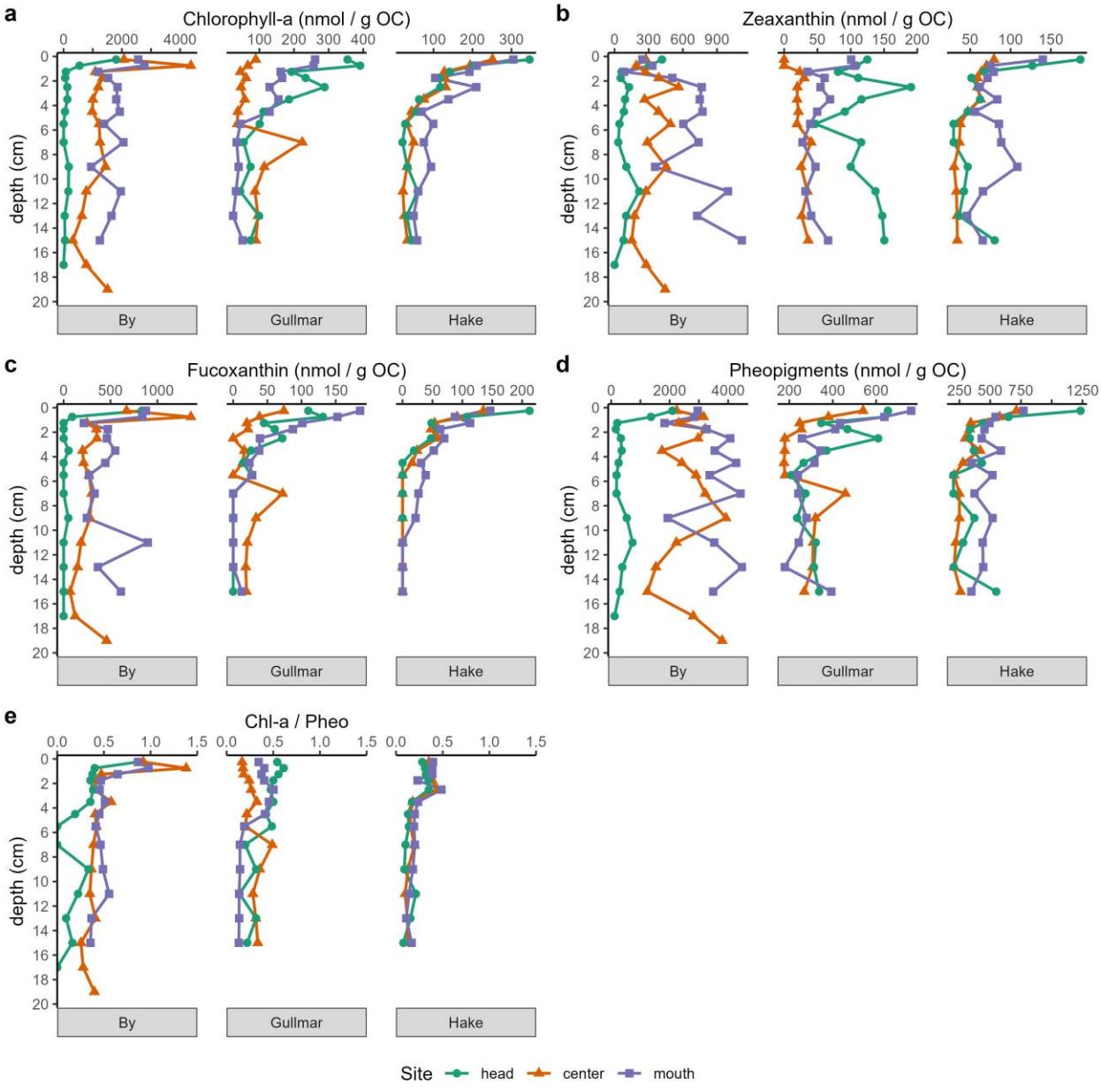

Figure 7. Downcore profiles of a) chlorophyll-a concentrations, b) zeaxanthin concentrations, c) fucoxanthin concentrations, d) pheo-pigment concentrations, and e) chlorophyll-a/pheopigment ratios (Chl-a/ pheo). Each subfigure is faceted by fjord and color coded by site.

4 Discussion

4.1 OC Sources and Burial

The average MAR and OCAR within all three western Swedish fjords increased from the head-to-mouth (Table 1, Figure 4). Highest MARs in fjords are commonly found adjacent to terrestrial inflow sources (e.g., rivers) and/or in deep basins where fine particulates (e.g., clays in soils) accumulate via hydrodynamic sorting (Á Norði et al., 2018; Cowie et al., 1992; Hinojosa et al., 2014). However, the elevated MARs at the mouth of the Swedish fjords reflects the role of the coastal ocean as an important source of particulate delivery. High spatial variability in OCARs in these fjords (Fig.4) agrees with patterns found in other fjord systems (Á Norði et al., 2018; Duffield et al., 2017; Ramirez et al., 2016), emphasizing the importance of head-to-mouth spatial dynamics in fjords. Average OCARs for By, Gullmar, and Hake Fjords were 13 ± 5 g OC m^{-2} yr^{-1}, 37 ± 12 g OC m^{-2} yr^{-1}, and 64 ± 20 g OC m^{-2} yr^{-1}, respectively, with a total average of 38 ± 25 g OC m^{-2} yr^{-1} (Table 1, Fig. 4). The average OCAR in this study are slightly higher than estimates for NW Europe (29 g OC m^{-2} yr^{-1}-; Cui, Bianchi, Savage, et al., 2016) but are relatively low compared to Norwegian temperate fjords (71 g OC m^{-2} yr^{-1}; Włodarska-Kowalczuk et al., 2019).

Fjords along western Sweden are characterized by an open exchange with coastal waters, minimal riverine inputs, low-relief, and burial of predominantly marine-derived OC. Of the total OC buried in this study, 83% is marine derived, equating to an average $OC_{mar}AR$ of 32 ± 21 g OC m^{-2} yr^{-1} (Fig. 4). This is much higher than previous estimates for NW Europe which suggested only 23.5% of the OC buried is marine derived (Cui, Bianchi, Savage, et al., 2016). The $\delta^{13}C$ mixing model values suggest fjords with no riverine input have high OC_{mar} contributions throughout the entire fjord (e.g. Hake Fjord with average 90 ± 2% OC_{mar}) while fjords with significant riverine inputs typically have steeper gradients of OC sources from the head-to-mouth (e.g. 47 ± 11% to 73 ± 11% OC_{mar} in By Fjord and 40 ± 10% to 87 ± 8% OC_{mar} in Gullmar Fjord; Fig. 3c). This implies that rivers, while not dominant sources of particulates to these fjords, are the dominant source of OC_{terr} to these systems. Mass wasting events are

dominant sources of OC_{terr} in high relief watersheds of New Zealand, Canadian, Chilean, and Alaskan fjords (Cui, Bianchi, Jaeger, et al., 2016; Cui et al., 2017; Hage et al., 2022; Korup et al., 2019; Ramirez et al., 2016). Landslides have been recorded in Swedish fjord sediments (Polovodova et al., 2011), but are likely not an important point source of OC_{terr} inputs to the fjords because of the relatively low relief of these fjord basins. Low OC_{terr} inputs are further supported by low Λ_8 concentrations as values ranged from 0.5 to 2.3 mg/100 mg OC while in other fjords (e.g. Saguenay Fjord (CA), Doubtful Sound (NZ), Dusky Sound (NZ), Long Sound (NZ)), Λ_8 concentrations reach 7.7 to 10.8 mg (100 mg OC)$^{-1}$ (Cui, Bianchi, Savage, et al., 2016; Louchouarn et al., 1997; Walsh et al., 2008). The dominance of OC_{mar} burial in these fjords supports the general paradigm that fjords with low riverine inputs and high marine inflow are typically dominated by OC_{mar} in sediments (Faust & Knies, 2019). In fact, marine inflow rates are much higher than riverine discharge rates in the fjords of this study. For instance, the Bäve and Örekil rivers, located at the heads of By and Gullmar Fjords, respectively, have discharges of 4-8 and 24 $m^3 s^{-1}$, respectively (Stigebrandt et al., 2015; Tiselius et al., 2016; Viktorsson et al., 2013). However, the net marine circulation through the Orust-Tjörn fjord system is considerably higher at 100 $m^3 s^{-1}$ and circulates counterclockwise in a northern direction, pushing coastal waters from the Skagerrak Straight and Kattegat Sea into these fjords (Björk et al., 2000). The strong inflow of marine water also likely restricts the OC_{terr} from being transported throughout the fjord while supplying high OC_{mar} loads to the system.

4.2 OC Decay Dynamics: Source Inputs, Redox, and Spatial Variability

4.2.1 Terrestrially-Derived OC

Spatial variability of OC_{terr} sources from head-to-mouth transects suggests that deposition of terrestrial material, while relatively minimal compared to marine sources, is strongly influenced by hydrodynamic sorting. For instance, Λ_8 values, a proxy for total OC_{terr} inputs, supports our bulk stable isotopic mixing model and highlights rivers as an important point source of OC_{terr} into these systems (Fig. 3c, Fig. 5a). Based on C/V and S/V ratios, OC_{terr} in By, Gullmar, and Hake Fjords is a mixture of woody and non-woody angiosperm and gymnosperm material (Fig. 5c, Fig. S5a-b). The dominant gymnosperm sources to fjords in this region are likely from pine trees and spruce trees and angiosperm sources from birch trees (Diekmann, 1999), all of which were observed while collecting terrestrial endmembers. At Gullmar-H and

By-H stations, which have direct riverine inputs at the head, OC_{terr} is more comprised of woody and gymnosperm material compared to all other sites (Fig. 5c, Fig. S5a-b). However, at the distal regions of By and Gullmar Fjords (By-C, By-M, Gullmar-C, Gullmar-M), and in the entire Hake Fjord, there are higher soil OC_{terr} contributions as reflected by higher 3,5-Bd/V ratios (Fig. S5d). This distribution of OC_{terr} throughout the fjord can be explained by hydrodynamic sorting, which has been reported as a key driver of OC_{terr} distribution in temperate fjords (Cui, Bianchi, Hutchings, et al., 2016; Loh et al., 2008; Smith et al., 2010; Walsh et al., 2008). Larger woody-plant material is deposited near rivers while smaller non-woody and fine soil material is preferentially transported to the distal regions of the fjord, also reflected by greater <63 μm fraction at sites not directly adjacent to rivers in Gullmar Fjord (Table 1). Non-point sources of soil erosion likely contributed to this signature as well, albeit only a minor contribution to the total OC pool.

Terrestrially-derived OC degradation patterns in sediments of western Swedish fjords are controlled more by distance from river mouth than water column redox conditions. The $(Ad/Al)_v$ and P/S+V ratios increase from head-to-mouth in Gullmar and By Fjords, while remaining relatively constant in Hake Fjord, suggesting greater degradation of OC_{terr} further from terrestrial point sources (e.g. rivers; Fig. 5b. Fig. S5c). Hydrodynamic sorting as previously described, is likely responsible for the spatial variation in OC_{terr} degradation wherein smaller more degraded vascular plant material is preferentially transported greater distances throughout the fjord, in contrast with fresh material being deposited at fjord heads. Elevated soil inputs at sites further away from rivers may also contribute to the more degraded terrestrial signature as soils typically display (Ad/Al)v ratios of 0.6 to 0.8 (Ertel & Hedges, 1984). Patterns of increasing OC_{terr} degradation moving away from terrestrial sources (e.g. riverine input) has similarly been reported in coastal systems (Bianchi, Mitra, et al., 2002; Prahl et al., 1994; Sampere et al., 2008) and fjords specifically (Cui, Bianchi, Savage, et al., 2016; Walsh et al., 2008). Stable Λ_8 and P/S+V values and increasing $(Ad/Al)_v$ ratios downcore at all sites excluding the By-H station indicates the relative stability of lignin in the sediments (Fig. 5a-b, Fig. S5c). This shows that OC_{terr} is not being diagenetically altered within the time scale of the 20 cm of the sediments (20 to 116 years), suggesting minimal post-depositional degradation of OC_{terr}. There is no significant difference in the degradation state of lignin between the anoxic stations of By Fjord (By-C and By-M), and oxic Hake Fjord stations (Hake-H, Hake-C, and Hake-M), suggesting pre-

depositional degradation is not controlled by water-column redox. The degraded signature of lignin likely reflects degradation of OC_{terr} prior to delivery into fjords (Hedges, Clark, et al., 1988; Louchouarn et al., 1997). While a low reactivity of lignin in water columns and sediments of fjords has been attributed to low oxygen levels (Cowie et al., 1992), we observed minimal decay of OC_{terr} in oxidizing water columns of West Swedish fjords.

4.2.2 Marine-Derived OC

Swedish fjords bury significant portions of the annual primary production regardless of water column redox state. The 10 year mean annual primary production in Gullmar Fjord from 1985 to 2008 ranged from 220 to 240 g OC m^{-2} yr^{-1} (Lindahl et al., 2009). We assume similar values for By and Hake Fjords since there are no published production estimates for them. Based on the average $OC_{mar}AR$, the anoxic By Fjord, seasonally hypoxic Gullmar Fjord, and oxic Hake Fjord bury ~4%, ~13%, and ~25% of the total annual primary production in surface waters, respectively. This agrees with estimates reported on subarctic and arctic fjords of Norway and Svalbard (10%) and temperate fjords of Norway (20%; Kuliński et al., 2014; Włodarska-Kowalczuk et al., 2019). Highest OC_{mar} burial efficiencies are in Hake Fjord which also has the highest MAR (Table 1), further supporting sediment accumulation rate as a key driver of OC burial in these fjords.

Marine-derived OC is similarly degraded under oxic, anoxic, and seasonally hypoxic water columns and experiences minimal post-depositional degradation, as reflected by THAA biomarkers which exhibit comparable profiles between sites and minimal changes downcore. While amino acids are ubiquitous in all living matter, they constitute the majority of the biomolecules in OC_{mar} compared to OC_{terr}, meaning they can be more representative of the marine end-member (Burdige, 2007; Wakeham et al., 1997). Based on mixing model results, we assume amino acids primarily derive from marine phytoplankton in this study. Amino acid biomarkers have not been extensively used in fjord systems, but the values reported here are comparable to values previously reported in Saanich Inlet, an intermittently anoxic fjord (Cowie et al., 1992), and St. Lawrence Estuary, a hypoxic fjord (Alkhatib et al., 2012). Bulk OC_{mar} is stable in the sediments post-deposition as the OC content and enriched $\delta^{13}C$ values are distinctly vertical at all sites (excluding By-H) to basal ages in sediment cores, ranging from 20 to 116 years (Fig. 3a-b). Moreover, minimal changes in amino acid biomarkers downcore at all sites

572 (excluding By-H) exhibit only slight degradation of OC_{mar} in sediments throughout the
573 timeframe captured by these sediment cores (Fig. 6, Fig. S3, Fig. S4). Similarly, DI values are
574 not statistically different between oxic (Gullmar-H, Hake-C, Hake-M) and anoxic sites (By-C
575 and By-M). Despite small differences between all sites, average DI scores fall between -0.6 to
576 0.1 (the DI scale ranges from -2 to 2; Dauwe et al., 1999), suggesting OC_{mar} is intermediately
577 degraded at all sites. This is contrary to other estuarine and coastal studies which reported higher
578 (fresher) amino acid DI scores in sediments under low oxygen and hypoxic water columns
579 (Alkhatib et al., 2012; Vandewiele et al., 2009; Wang et al., 2018). Amino acids have been found
580 to be reactive in fjord water columns, suggesting the THAA DI can reflect pre-depositional
581 degradation as material sinks through the water column (Cowie et al., 1992). Concentrations of
582 THAA in surface sediments are remarkably similar between long-term oxic sites (Hake-C and
583 Hake-M), seasonally hypoxic sites (Gullmar-C), and long-term anoxic sites (By-C and By-M;
584 Fig. 6a). Assuming similar primary production rates (and therefore amino acid inputs), as
585 mentioned above, such similar THAA concentrations and DI values of sediments under different
586 water-column redox states and depths suggest OC_{mar} is similarly processed under various water
587 column oxygen conditions. Therefore, OC_{mar} is similarly preserved under long-term oxic,
588 seasonally hypoxic, and long-term anoxic water columns in these settings.
589 Interestingly, pigment concentrations (another labile OC biomarker), showed variable
590 preservation across different water column redox conditions that were not observed with amino
591 acids. At the anoxic stations within By Fjord, pigment concentrations are one order of magnitude
592 higher and therefore better preserved down to 20 cm sediment depth than in the seasonally
593 hypoxic and oxic stations of Gullmar and Hake Fjords (Fig. 7a-c). Chlorophyll-a/pheopigment
594 ratios also suggest greatest preservation of OC_{mar} at the anoxic stations (By-C and By-M; Fig.
595 7d), agreeing with the importance of anoxia on pigment preservation (Bianchi et al., 2000; Jessen
596 et al., 2017; Reuss et al., 2005; Sun et al., 1993; Szymczak-Żyła et al., 2017). Large differences
597 in pigment concentrations between anoxic and seasonally hypoxic/oxic stations suggest greatest
598 OC_{mar} contributions and preservation in By Fjord. However, this contradicts bulk OC, stable
599 isotope, and amino acid biomarker profiles at oxic and seasonally hypoxic stations of Hake and
600 Gullmar Fjords. The discrepancy between pigment biomarkers versus bulk OC and amino acid
601 biomarkers is likely due to the lability of pigment biomarkers and their susceptibility to both
602 biotic and abiotic degradation. Previous work in the fjords of New Zealand (Schüller & Savage,

603 2011) and the fjords of the Baltic Sea (Bianchi, Engelhaupt, et al., 2002) have proven disparities
604 between water column phytoplankton communities and sedimentary pigment concentrations.
605 Such discrepancies may arise from a variety of factors including but not limited to different
606 reactivities of pigment classes, bioturbation, oxygen levels, grazing, microbial decay, sediment
607 resuspension, and photooxidation (Bianchi, Engelhaupt, et al., 2002; Schüller & Savage, 2011).
608 However, are useful in conjunction with other proxies and may still be applicable to determine
609 the presence of certain phytoplankton classes (Bianchi, Engelhaupt, et al., 2002; Schüller &
610 Savage, 2011). The presence of fucoxanthin in surface sediments of our study sites confirms
611 diatom biomass is being delivered to the benthos and the presence of zeaxanthin suggests
612 cyanobacterial contributions to the sediments. Numerous studies in Gullmar Fjord identify
613 diatoms and dinoflagellates as the main phytoplankton species (Belgrano et al., 1999; Waite et
614 al., 2005) and they are likely the main sources of OC_{mar} in By and Hake Fjords as well as they
615 are in close proximity to Gullmar Fjord.

616 ### 4.3 Drivers of OC Preservation in Fjords

617 #### 4.3.1 Water Column Redox and Oxygen Exposure Time

618 Overall similarities in OC degradation state in surface sediments and downcore and at all
619 sites, despite variable water column redox states, suggest water column redox is not a primary
620 driver of OC degradation in these systems. Based on bottom water oxygen concentrations and
621 sediment oxygen uptake rates measured using benthic chamber landers during the same Sept.-
622 Oct. 2021 cruise, the fall oxygen penetration depth (OPD) was shallow at 0 mm, 16.7 to 20.0
623 mm, and 10.7 to 12.3 mm in By, Gullmar, and Hake Fjord center stations, respectively.
624 Calculating the sedimentary oxygen exposure time (OET; Text S2) from linear sedimentation
625 rates and OPDs, the OET in fall in By, Gullmar, and Hake Fjords is 0 months, 5.1 to 6.1 months,
626 and 3.7 to 4.2 months, respectively. It is important to note these calculations are available for
627 center stations only and are only applicable to the time of sampling. These OETs are shorter than
628 those reported for the St. Lawrence Estuary (1 to 14 years; Alkhatib et al., 2012). With such
629 short sedimentary OETs due to high OC loads and high sediment accumulation rates (Alkhatib et
630 al., 2012), it is likely that the OC in these systems is not exposed to the water column redox
631 conditions long enough for differential degradation to occur. The material appears to be quickly
632 removed from the water column redox conditions—whether anoxic, oxic, or seasonally

hypoxic— to an anoxic environment in surface sediments where degradation occurs slowly. High OC:SA ratios (>1 mg OC m^{-2}, except at Gullmar-C where the OC:SA ratio is 0.9 mg OC m^{-2}) reported for surface sediments at oxic, hypoxic, and anoxic sites further supports minimal decomposition across the redox gradient due to low OET (Table 1; Blair & Aller, 2012). Moreover, Ox/Anox ratios are not statistically different between sites with long-term anoxic, seasonally hypoxic, and long oxic water columns with all averages being less than 1.5 (excluding site Gullmar-C), suggesting the material was minimally degraded in aerobic settings at all sites; Fig. S3b). Therefore, water column redox state is not an important driver of OC degradation in these fjords. The low OC content, Λ_8 concentrations and THAA concentrations and higher degradation reflected by mol % BALA and $(Ad/Al)_v$ at By-H compared to all other sites (Fig. 5a-b, Fig. 6a, Fig. S3) is likely due to the oxic water column but low MAR which does not result in a low OET. Similar findings by Cowie and Hedges (1992) showed remarkably similar preservation of numerous biochemicals in Dabob Bay (oxic) and Saanich Inlet (anoxic), suggesting sedimentation rate rather than bottom water O_2 concentration controls preservation. High sediment accumulation rates and high OC loads are common in fjords globally (Bianchi et al., 2020), so other well-ventilated fjords, such as those recorded in Scotland, Norway, New Zealand, Chile, Canada (Carter, 1976; Faust & Knies, 2019; Jackson et al., 2021; Silva & Vargas, 2014; Smeaton et al., 2021), likely also have shallow OPDs and short OETs which promotes high OC burial efficiencies, even of labile marine-derived OC.

Comparable degradation states of OC, as indicated by THAA and lignin biomarkers, are observed across sites with surface mixed layers (SMLs) ranging from 0 to 12 cm (Table 1, Fig. 5b, 6b). This implies that the intensity and frequency of sediment mixing in these fjords, caused by physical or biological processes, does not stimulate OC degradation in these sediments. Bioturbation and SMLs can greatly influence OC degradation as it can re-oxidize the sediments thus increasing the OET, cause oscillations in redox state that stimulate microbial communities, and mix labile OC deeper which may cause priming effects (Bianchi, 2011; Middelburg, 2018). The importance of priming, while difficult to identify in aquatic systems (Bengtsson et al., 2014; Bianchi, 2011; Guenet et al., 2010), has been shown to exist in coastal sediments (Aller & Cochran, 2019; Van Nugteren et al., 2009). Using the linear sediment accumulation rate and SML depth to calculate residence time in the SML, particle residence times in the SML range from ~4 to ~42 years throughout the three fjords. Even spanning decadal differences in residence

times within the SML (including no SML), OC degradation state (e.g., DI and $(Ad/Al)_v$), OC:SA ratios) fall within the same broad categories which suggest sediment mixing does not alter OC preservation in these systems. Negligible effects of SML depth on OC content has been reported in other fjords (Cui, Bianchi, Savage, et al., 2016). This may be linked to the shallow OPD in fjord systems globally—there is a high oxygen demand in the sediments due to high OC loads, thus any oxygen introduced into the sediments is quickly consumed. Similar Ox/Anox ratios between sites regardless of SML depth and water column redox supports the notion that surface mixing did not increase OET in sediments (Fig. S3b**).**

Quick sinking of phytoplankton material through Swedish fjord water columns shortens pre-depositional OETs and likely contributes to efficient OC_{mar} burial. Large differences of surface sediment pigment concentrations between anoxic sites (By-C and By-M) versus oxic/seasonally hypoxic (Hake-H, -C, -M, Gullmar-H, -C, -M) sites during the fall sampling campaign suggests some degree of pre-depositional processing of phytoplankton material is occurring as material sinks through oxidizing water columns (Fig. 7a-c). While redox and pigment preservation are clearly coupled (see section 4.2.2), another plausible explanation may be enhanced zooplankton heterotrophy during the time of sampling which promotes OC sinking in Hake and Gullmar Fjords. However, in the absence of sediment trap data, we can only speculate at this time. Inflows of Skagerrak into Gullmar Fjord have been linked to higher zooplankton biomass in fall (Lindahl & Hernroth, 1988), and Gullmar and Hake Fjords are much more connected to the Skagerrak than By Fjord (Fig. 1). Previous work in Gullmar Fjord has highlighted the importance of zooplankton grazing on phytoplankton-derived carbon fluxes to the benthos in summer and fall (Calliari & Tiselius, 2009; Tiselius et al., 2012; Vargas et al., 2002), accounting for approximately 11.4% of the primary production export (Vargas et al., 2002). Such grazing by copepods would alter pigment structures to more stable carotenol chlorin esters (CCEs) and steryl chlorin esters (SCEs) (Chen et al., 2003; Goericke et al., 1999; Harradine et al., 1996) while also facilitating sinking of phytoplankton material. Efficient burial of OC_{mar} just after the spring bloom is also plausible and likely also contributes to high OC_{mar}AR. Previous research in Gullmar Fjord identified diatoms as the main sinking material in spring with 63 to 189% of primary production sinking ungrazed from surface waters because of aggregation and quick sinking of diatom material (Tiselius & Kuylenstierna, 1996; Waite et al.,

2005). Variable mechanisms of quick sinking of OC_{mar} year-round likely contributed to high sediment and OC accumulation rates.

4.3.2 Marine-Dominated Fjords: Implications for Carbon Burial

Marine-dominated fjords are particularly efficient carbon sinks when compared to OC_{terr} or OC_{petro} dominated fjords as the carbon stored in sediments, deriving from both autochthonous and allochthonous phytoplankton biomass, is "new" carbon that follows a more direct path from CO_2 to phytoplankton biomass (even in the form of zooplankton pellets or houses) to burial in sediments. In marine-dominated fjords, significant portions of primary production are effectively buried (~14% to 20%; this study and Włodarska-Kowalczuk et al., 2019) whereas only a very small fraction is effectively buried in other marine and coastal systems (0.25% and <1.3%, respectively; Burdige, 2005). While OC_{terr} is also minimally degraded in the fjord system, the allochthonous carbon has been removed from the atmosphere elsewhere and has a long residence time in an oxidizing terrestrial biosphere where it is susceptible to aerobic decomposition and mineralization prior to deposition/burial in fjords. Moreover, OC_{terr} is likely to be stored in coastal sediments regardless of deposition in fjords because of its propensity for high burial efficiency in continental margin and marine sediments (44 and 36%, respectively; Burdige, 2005). Similarly, allochthonous OC_{petro} buried in fjord sediments is carbon that has already been removed from the atmosphere over geologic timescales. The reintroduction of OC_{petro} to the modern carbon cycle via erosion may actually allow OC_{petro} to be a net carbon source, based on recent work showing that microbes are capable of consuming OC_{petro} along the aquatic continuum (Kim et al., 2023; Ruben et al., 2023). In this case, storage of OC_{terr} and OC_{petro} in fjord sediments, while still important in carbon sequestration, is secondary burial as it is carbon that has already been removed from the atmosphere. Early work predicted that fjords of NW Europe are terrestrially dominated (Cui, Bianchi, Savage, et al., 2016). However, as more research is conducted on the fjords of NW Europe, including in Sweden (this study), Norway, Scotland and the Faroe Islands, there is growing evidence that many fjords in the region are burying mostly OC_{mar} (Á Norði et al., 2018; Faust & Knies, 2019; Smeaton et al., 2021; Włodarska-Kowalczuk et al., 2019). With such high OC_{mar} burial rates, fjords of NW Europe are likely hotspots for carbon sequestration, via phytoplankton at the air-water interface, to subsequent burial.

5 Conclusions

This study examined the effect of water-column redox on OC burial in Swedish temperate fjord sediments using a multi-biomarker and stable isotopic approach to characterize the sources and degradation state of OC in these sediments. The fjords in this study, including the By, Gullmar, and Hake Fjords, had average OCARs that are comparable to other temperate fjords. Rivers are important point sources of OC_{terr} into Swedish fjords, but these systems bury primarily OC_{mar} under various redox conditions. It is likely that OC_{mar} burial rates are underestimated in fjords globally. Lignin and THAA biomarkers reflect similar degradation states of OC_{mar} and OC_{terr} in fjords with long-term anoxic, seasonally hypoxic, and long-term oxic water columns which results in similar bulk OC content downcore. The key drivers of OC burial in Swedish fjords are therefore high sediment accumulation rates and high OC loads which result in short sediment OETs and quick burial of OC. It is important to note that other forms of OC stabilization not discussed here, such as mineral associations, may also play an important role in OC preservation and burial in fjords. The results presented here illustrate a decoupling of system redox and OC source with OC degradation state which emphasizes fjords as hotspots of labile OC burial. With anthropogenic induced global change, we can expect to see changes in coastal oxygenation, terrestrial sediment and OC delivery, as well as marine primary production, so it is imperative to study how such drivers influence the role of aquatic critical zones in the global carbon cycle (Bauer et al., 2013; Bianchi & Morrison, 2018; Breitburg et al., 2018).

Acknowledgments

We would like to thank Jason Curtis for bulk and isotopic measurements, Mikhail Kononets for benthic oxygen flux data, Andrew Zimmerman for sediment surface area analysis, and the crew of the University of Gothenburg R/V Skagerrak and scientists on board for sampling assistance. Support for laboratory analysis was provided by the Jon and Beverly Thompson Chair in the Department of Geological Sciences at the University of Florida and travel support was provided by the Department of Geological Sciences, the Center for European Studies, the Land Use and Environmental Change Institute, and the College of Liberal Arts and Sciences at the University of Florida. The ship expedition was financed by funding from the Swedish Agency for Marine

and Water Management (HaV) to POJH. We would like to thank David Burdige, Jorien E. Vonk, and one anonymous reviewer for their constructive feedback during the review process.

Open Research

Data for this study is available in supplemental files. Bottom water dissolved oxygen data for each fjord is available at https://sharkweb.smhi.se/.

References

Á Norði, G., Glud, R. N., Simonsen, K., & Gaard, E. (2018). Deposition and benthic mineralization of organic carbon: A seasonal study from Faroe Islands. *Journal of Marine Systems*, *177*, 53–61. https://doi.org/10.1016/j.jmarsys.2016.09.005

Alkhatib, M., Schubert, C. J., Del Giorgio, P. A., Gelinas, Y., & Lehmann, M. F. (2012). Organic matter reactivity indicators in sediments of the St. Lawrence Estuary. *Estuarine, Coastal and Shelf Science*, *102–103*, 36–47. https://doi.org/10.1016/j.ecss.2012.03.002

Aller, R. C., & Cochran, J. K. (2019). The Critical Role of Bioturbation for Particle Dynamics, Priming Potential, and Organic C Remineralization in Marine Sediments: Local and Basin Scales. *Frontiers in Earth Science*, *7*, 157. https://doi.org/10.3389/feart.2019.00157

Appleby, P. G., & Oldfield, F. (1978). The calculation of lead-210 dates assuming a constant rate of supply of unsupported 210Pb to the sediment. *CATENA*, *5*(1), 1–8. https://doi.org/10.1016/S0341-8162(78)80002-2

Arndt, S., Jørgensen, B. B., LaRowe, D. E., Middelburg, J. J., Pancost, R. D., & Regnier, P. (2013). Quantifying the degradation of organic matter in marine sediments: A review and synthesis. *Earth-Science Reviews*, *123*, 53–86. https://doi.org/10.1016/j.earscirev.2013.02.008

Arnold, S. L., & Schepers, J. S. (2004). A Simple Roller-Mill Grinding Procedure for Plant and Soil Samples. *Communications in Soil Science and Plant Analysis*, *35*(3–4), 537–545. https://doi.org/10.1081/CSS-120029730

Bauer, J. E., Cai, W.-J., Raymond, P. A., Bianchi, T. S., Hopkinson, C. S., & Regnier, P. A. G. (2013). The changing carbon cycle of the coastal ocean. *Nature*, *504*(7478), 61–70. https://doi.org/10.1038/nature12857

780 Belgrano, A., Lindahl, O., & Hernroth, B. (1999). North Atlantic Oscillation primary productivity and toxic
781 phytoplankton in the Gullmar Fjord, Sweden (1985–1996). *Proceedings of the Royal Society of London.*
782 *Series B: Biological Sciences*, *266*(1418), 425–430. https://doi.org/10.1098/rspb.1999.0655
783 Bengtsson, M. M., Wagner, K., Burns, N. R., Herberg, E. R., Wanek, W., Kaplan, L. A., & Battin, T. J. (2014). No
784 evidence of aquatic priming effects in hyporheic zone microcosms. *Scientific Reports*, *4*(1), 5187.
785 https://doi.org/10.1038/srep05187
786 Bianchi, T. S. (2011). The role of terrestrially derived organic carbon in the coastal ocean: A changing paradigm and
787 the priming effect. *Proceedings of the National Academy of Sciences*, *108*(49), 19473–19481.
788 https://doi.org/10.1073/pnas.1017982108
789 Bianchi, T. S., & Canuel, E. A. (2011). *Chemical biomarkers in aquatic ecosystems*. Princeton: Princeton University
790 Press.
791 Bianchi, T. S., & Morrison, E. (2018). Human Activities Create Corridors of Change in Aquatic Zones. *Eos*, *99*.
792 https://doi.org/10.1029/2018EO104743
793 Bianchi, T. S., Johansson, B., & Elmgren, R. (2000). Breakdown of phytoplankton pigments in Baltic sediments:
794 effects of anoxia and loss of deposit-feeding macrofauna. *Journal of Experimental Marine Biology and*
795 *Ecology*, *251*(2), 161–183. https://doi.org/10.1016/S0022-0981(00)00212-4
796 Bianchi, T. S., Engelhaupt, E., McKee, B. A., Miles, S., Elmgren, R., Hajdu, S., et al. (2002). Do sediments from
797 coastal sites accurately reflect time trends in water column phytoplankton? A test from Himmerfjärden Bay
798 (Baltic Sea proper). *Limnology and Oceanography*, *47*(5), 1537–1544.
799 https://doi.org/10.4319/lo.2002.47.5.1537
800 Bianchi, T. S., Mitra, S., & McKee, B. A. (2002). Sources of terrestrially-derived organic carbon in lower
801 Mississippi River and Louisiana shelf sediments: implications for differential sedimentation and transport
802 at the coastal margin. *Marine Chemistry*, *77*(2–3), 211–223. https://doi.org/10.1016/S0304-4203(01)00088-
803 3
804 Bianchi, T. S., Schreiner, K. M., Smith, R. W., Burdige, D. J., Woodard, S., & Conley, D. J. (2016). Redox Effects
805 on Organic Matter Storage in Coastal Sediments During the Holocene: A Biomarker/Proxy Perspective.
806 *Annual Review of Earth and Planetary Sciences*, *44*(1), 295–319. https://doi.org/10.1146/annurev-earth-
807 060614-105417

Bianchi, T. S., Cui, X., Blair, N. E., Burdige, D. J., Eglinton, T. I., & Galy, V. (2018). Centers of organic carbon burial and oxidation at the land-ocean interface. *Organic Geochemistry*, *115*, 138–155. https://doi.org/10.1016/j.orggeochem.2017.09.008

Bianchi, T. S., Arndt, S., Austin, W. E. N., Benn, D. I., Bertrand, S., Cui, X., et al. (2020). Fjords as aquatic critical zones (ACZs). *Earth-Science Reviews*, *203*, 103145. https://doi.org/10.1016/j.earscirev.2020.103145

Björk, G., Liungman, O., Rydberg, L., & Bjork, G. (2000). Net Circulation and Salinity Variations in an Open-Ended Swedish Fjord System. *Estuaries*, *23*(3), 367. https://doi.org/10.2307/1353329

Blair, N. E., & Aller, R. C. (2012). The Fate of Terrestrial Organic Carbon in the Marine Environment. *Annual Review of Marine Science*, *4*(1), 401–423. https://doi.org/10.1146/annurev-marine-120709-142717

Bourgeois, S., Kerhervé, P., Calleja, M. Ll., Many, G., & Morata, N. (2016). Glacier inputs influence organic matter composition and prokaryotic distribution in a high Arctic fjord (Kongsfjorden, Svalbard). *Journal of Marine Systems*, *164*, 112–127. https://doi.org/10.1016/j.jmarsys.2016.08.009

Breitburg, D., Levin, L. A., Oschlies, A., Grégoire, M., Chavez, F. P., Conley, D. J., et al. (2018). Declining oxygen in the global ocean and coastal waters. *Science*, *359*(6371), eaam7240. https://doi.org/10.1126/science.aam7240

Brinkmann, I., Barras, C., Jilbert, T., Næraa, T., Paul, K. M., Schweizer, M., & Filipsson, H. L. (2022). Drought recorded by Ba/Ca in coastal benthic foraminifera. *Biogeosciences*, *19*(9), 2523–2535. https://doi.org/10.5194/bg-19-2523-2022

Burdige, D. J. (2005). Burial of terrestrial organic matter in marine sediments: A re-assessment: terrestrial organic matter in marine sediments. *Global Biogeochemical Cycles*, *19*(4), n/a-n/a. https://doi.org/10.1029/2004GB002368

Burdige, D. J. (2007). Preservation of Organic Matter in Marine Sediments: Controls, Mechanisms, and an Imbalance in Sediment Organic Carbon Budgets? *Chemical Reviews*, *107*(2), 467–485. https://doi.org/10.1021/cr050347q

Cai, W.-J., & Sayles, F. L. (1996). Oxygen penetration depths and fluxes in marine sediments. *Marine Chemistry*, *52*(2), 123–131. https://doi.org/10.1016/0304-4203(95)00081-X

834 Calliari, D., & Tiselius, P. (2009). Organic carbon fluxes through the mesozooplankton and their variability at
835 different time-scales in the Gullmarsfjord, Sweden. *Estuarine, Coastal and Shelf Science*, *85*(1), 107–117.
836 https://doi.org/10.1016/j.ecss.2009.06.016
837 Calvin, K., Dasgupta, D., Krinner, G., Mukherji, A., Thorne, P. W., Trisos, C., et al. (2023). *IPCC, 2023: Climate*
838 *Change 2023: Synthesis Report. Contribution of Working Groups I, II and III to the Sixth Assessment*
839 *Report of the Intergovernmental Panel on Climate Change [Core Writing Team, H. Lee and J. Romero*
840 *(eds.)]. IPCC, Geneva, Switzerland.* (First). Intergovernmental Panel on Climate Change (IPCC).
841 https://doi.org/10.59327/IPCC/AR6-9789291691647
842 Carter, L. (1976). Seston transport and deposition in Pelorus sound, south Island, New Zealand. *New Zealand*
843 *Journal of Marine and Freshwater Research*, *10*(2), 263–282.
844 https://doi.org/10.1080/00288330.1976.9515612
845 Chen, N., Bianchi, T. S., & Bland, J. M. (2003). Novel decomposition products of chlorophyll-a in continental shelf
846 (Louisiana shelf) sediments: formation and transformation of carotenol chlorin esters. *Geochimica et*
847 *Cosmochimica Acta*, *67*(11), 2027–2042. https://doi.org/10.1016/S0016-7037(02)01297-8
848 Cowie, G.L., & Hedges, J. I. (1992). The role of anoxia in organic matter preservation in coastal sediments: relative
849 stabilities of the major biochemicals under oxic and anoxic depositional conditions. *Organic Geochemistry*,
850 *19*(1–3), 229–234. https://doi.org/10.1016/0146-6380(92)90039-Z
851 Cowie, G.L., Hedges, J. I., Prahl, F. G., & de Lange, G. J. (1995). Elemental and major biochemical changes across
852 an oxidation front in a relict turbidite: An oxygen effect. *Geochimica et Cosmochimica Acta*, *59*(1), 33–46.
853 https://doi.org/10.1016/0016-7037(94)00329-K
854 Cowie, Gregory L., & Hedges, J. I. (1992). Sources and reactivities of amino acids in a coastal marine environment.
855 *Limnology and Oceanography*, *37*(4), 703–724. https://doi.org/10.4319/lo.1992.37.4.0703
856 Cowie, Gregory L., & Hedges, J. I. (1994). Biochemical indicators of diagenetic alteration in natural organic matter
857 mixtures. *Nature*, *369*(6478), 304–307. https://doi.org/10.1038/369304a0
858 Cowie, Gregory L, Hedges, J. I., & Calvert, S. E. (1992). Sources and relative reactivities of amino acids, neutral
859 sugars, and lignin in an intermittently anoxic marine environment. *Geochimica et Cosmochimica Acta*,
860 *56*(5), 1963–1978. https://doi.org/10.1016/0016-7037(92)90323-B

Cui, X., Bianchi, T. S., Jaeger, J. M., & Smith, R. W. (2016). Biospheric and petrogenic organic carbon flux along southeast Alaska. *Earth and Planetary Science Letters*, *452*, 238–246. https://doi.org/10.1016/j.epsl.2016.08.002

Cui, X., Bianchi, T. S., Savage, C., & Smith, R. W. (2016). Organic carbon burial in fjords: Terrestrial versus marine inputs. *Earth and Planetary Science Letters*, *451*, 41–50.

Cui, X., Bianchi, T. S., Hutchings, J. A., Savage, C., & Curtis, J. H. (2016). Partitioning of organic carbon among density fractions in surface sediments of Fiordland, New Zealand: Density Fractionation. *Journal of Geophysical Research: Biogeosciences*, *121*(3), 1016–1031. https://doi.org/10.1002/2015JG003225

Cui, X., Bianchi, T. S., & Savage, C. (2017). Erosion of modern terrestrial organic matter as a major component of sediments in fjords. *Geophysical Research Letters*, *44*(3), 1457–1465. https://doi.org/10.1002/2016GL072260

Cui, X., Mucci, A., Bianchi, T. S., He, D., Vaughn, D., Williams, E. K., et al. (2022). Global fjords as transitory reservoirs of labile organic carbon modulated by organo-mineral interactions. *Science Advances*, *8*(46), eadd0610. https://doi.org/10.1126/sciadv.add0610

Dauwe, B., & Middelburg, J. J. (1998). Amino acids and hexosamines as indicators of organic matter degradation state inNorth Sea sediments. *Limnology and Oceanography*, *43*(5), 782–798. https://doi.org/10.4319/lo.1998.43.5.0782

Dauwe, B., Middelburg, J. J., Herman, P. M. J., & Heip, C. H. R. (1999). Linking diagenetic alteration of amino acids and bulk organic matter reactivity. *Limnology and Oceanography*, *44*(7), 1809–1814. https://doi.org/10.4319/lo.1999.44.7.1809

Diekmann, M. (1999). Southern deciduous forest. In H. Rydin & E. van der Maarel (Eds.), *Swedish plant geography: dedicated to Eddy van der Maarel on his 65th birthday*. Uppsala: Svenska Växtgeografiska Sällskapet.

Duffield, C., Alve, E., Andersen, N., Andersen, T., Hess, S., & Strohmeier, T. (2017). Spatial and temporal organic carbon burial along a fjord to coast transect: A case study from Western Norway. *The Holocene*, *27*(9), 1325–1339. https://doi.org/10.1177/0959683617690588

Ehinger, S. C., Pacer, R. A., & Romines, F. L. (1986). Separation of the radioelements210Pb−210Bi−210Po by spontaneous deposition onto noble metals and verification by Cherenkov and liquid scintillation counting.

Journal of Radioanalytical and Nuclear Chemistry Articles, *98*(1), 39–48. https://doi.org/10.1007/BF02060431

Ertel, J. R., & Hedges, J. I. (1984). The lignin component of humic substances: Distribution among soil and sedimentary humic, fulvic, and base-insoluble fractions. *Geochimica et Cosmochimica Acta*, *48*(10), 2065–2074. https://doi.org/10.1016/0016-7037(84)90387-9

Faust, J. C., & Knies, J. (2019). Organic Matter Sources in North Atlantic Fjord Sediments. *Geochemistry, Geophysics, Geosystems*, *20*(6), 2872–2885. https://doi.org/10.1029/2019GC008382

Filipsson, H. L., & Nordberg, K. (2004). Climate variations, an overlooked factor influencing the recent marine environment. An example from Gullmar Fjord, Sweden, illustrated by benthic foraminifera and hydrographic data. *Estuaries*, *27*(5), 867–881. https://doi.org/10.1007/BF02912048

Flynn, W. W. (1968). The determination of low levels of polonium-210 in environmental materials. *Analytica Chimica Acta*, *43*, 221–227. https://doi.org/10.1016/S0003-2670(00)89210-7

Gaye, B., Lahajnar, N., Harms, N., Paul, S. A. L., Rixen, T., & Emeis, K.-C. (2022). What can we learn from amino acids about oceanic organic matter cycling and degradation? *Biogeosciences*, *19*(3), 807–830. https://doi.org/10.5194/bg-19-807-2022

Goericke, R., Shankle, A., & Repeta, D. J. (1999). Novel carotenol chlorin esters in marine sediments and water column particulate matter. *Geochimica et Cosmochimica Acta*, *63*(18), 2825–2834. https://doi.org/10.1016/S0016-7037(99)00155-6

Goñi, M. A., & Hedges, J. I. (1995). Sources and reactivities of marine-derived organic matter in coastal sediments as determined by alkaline CuO oxidation. *Geochimica et Cosmochimica Acta*, *59*(14), 2965–2981. https://doi.org/10.1016/0016-7037(95)00188-3

Gruber, N., Bakker, D. C. E., DeVries, T., Gregor, L., Hauck, J., Landschützer, P., et al. (2023). Trends and variability in the ocean carbon sink. *Nature Reviews Earth & Environment*, *4*(2), 119–134. https://doi.org/10.1038/s43017-022-00381-x

Guenet, B., Danger, M., Abbadie, L., & Lacroix, G. (2010). Priming effect: bridging the gap between terrestrial and aquatic ecology. *Ecology*, *91*(10), 2850–2861. https://doi.org/10.1890/09-1968.1

915 Hage, S., Galy, V. V., Cartigny, M. J. B., Heerema, C., Heijnen, M. S., Acikalin, S., et al. (2022). Turbidity Currents
916 Can Dictate Organic Carbon Fluxes Across River-Fed Fjords: An Example From Bute Inlet (BC, Canada).
917 *Journal of Geophysical Research: Biogeosciences*, *127*(6). https://doi.org/10.1029/2022JG006824
918 Harradine, P. J., Harris, P. G., Head, R. N., Harris, R. P., & Maxwell, J. R. (1996). Steryl chlorin esters are formed
919 by zooplankton herbivory. *Geochimica et Cosmochimica Acta*, *60*(12), 2265–2270.
920 https://doi.org/10.1016/0016-7037(96)00132-9
921 Harris, D., Horwáth, W. R., & van Kessel, C. (2001). Acid fumigation of soils to remove carbonates prior to total
922 organic carbon or CARBON-13 isotopic analysis. *Soil Science Society of America Journal*, *65*(6), 1853–
923 1856. https://doi.org/10.2136/sssaj2001.1853
924 Hartnett, H. E., Keil, R. G., Hedges, J. I., & Devol, A. H. (1998). Influence of oxygen exposure time on organic
925 carbon preservation in continental margin sediments. *Nature*, *391*(6667), 572–575.
926 https://doi.org/10.1038/35351
927 Haugen, J.-E., & Lichtentaler, R. (1991). Amino acid diagenesis, organic carbon and nitrogen mineralization in
928 surface sediments from the inner Oslofjord, Norway. *Geochimica et Cosmochimica Acta*, *55*(6), 1649–
929 1661. https://doi.org/10.1016/0016-7037(91)90136-S
930 Hedges, J. I., & Ertel, J. R. (1982). Characterization of lignin by gas capillary chromatography of cupric oxide
931 oxidation products. *Analytical Chemistry*, *54*(2), 174–178. https://doi.org/10.1021/ac00239a007
932 Hedges, J. I., & Mann, D. C. (1979). The characterization of plant tissues by their lignin oxidation products.
933 *Geochimica et Cosmochimica Acta*, *43*(11), 1803–1807. https://doi.org/10.1016/0016-7037(79)90028-0
934 Hedges, J. I., Blanchette, R. A., Weliky, K., & Devol, A. H. (1988). Effects of fungal degradation on the CuO
935 oxidation products of lignin: A controlled laboratory study. *Geochimica et Cosmochimica Acta*, *52*(11),
936 2717–2726. https://doi.org/10.1016/0016-7037(88)90040-3
937 Hedges, J. I., Clark, W. A., & Come, G. L. (1988). Fluxes and reactivities of organic matter in a coastal marine bay.
938 *Limnology and Oceanography*, *33*(5), 1137–1152. https://doi.org/10.4319/lo.1988.33.5.1137
939 Henricsson, F., Ranebo, Y., Holm, E., & Roos, P. (2011). Aspects on the analysis of 210Po. *Journal of*
940 *Environmental Radioactivity*, *102*(5), 415–419. https://doi.org/10.1016/j.jenvrad.2010.09.010

941 Hinojosa, J. L., Moy, C. M., Stirling, C. H., Wilson, G. S., & Eglinton, T. I. (2014). Carbon cycling and burial in
942 New Zealand's fjords. *Geochemistry, Geophysics, Geosystems*, *15*(10), 4047–4063.
943 https://doi.org/10.1002/2014GC005433
944 Jackson, J. M., Bianucci, L., Hannah, C. G., Carmack, E. C., & Barrette, J. (2021). Deep Waters in British Columbia
945 Mainland Fjords Show Rapid Warming and Deoxygenation From 1951 to 2020. *Geophysical Research*
946 *Letters*, *48*(3), e2020GL091094. https://doi.org/10.1029/2020GL091094
947 Jessen, G. L., Lichtschlag, A., Ramette, A., Pantoja, S., Rossel, P. E., Schubert, C. J., et al. (2017). Hypoxia causes
948 preservation of labile organic matter and changes seafloor microbial community composition (Black Sea).
949 *Science Advances*, *3*(2), e1601897. https://doi.org/10.1126/sciadv.1601897
950 Jex, C. N., Pate, G. H., Blyth, A. J., Spencer, R. G. M., Hernes, P. J., Khan, S. J., & Baker, A. (2014). Lignin
951 biogeochemistry: from modern processes to Quaternary archives. *Quaternary Science Reviews*, *87*, 46–59.
952 https://doi.org/10.1016/j.quascirev.2013.12.028
953 Kim, D., Kim, J.-H., Ahn, Y., Jang, K., Jung, J. Y., Bae, M., & Nam, S.-I. (2023). Large contributions of petrogenic
954 and aged soil-derived organic carbon to Arctic fjord sediments in Svalbard. *Scientific Reports*, *13*(1),
955 17935. https://doi.org/10.1038/s41598-023-45141-z
956 King, L. L., & Repeta, D. J. (1991). Novel pyropheophorbide steryl esters in Black Sea sediments. *Geochimica et*
957 *Cosmochimica Acta*, *55*(7), 2067–2074. https://doi.org/10.1016/0016-7037(91)90044-6
958 Kononets, M., Tengberg, A., Nilsson, M., Ekeroth, N., Hylén, A., Robertson, E. K., et al. (2021). In situ incubations
959 with the Gothenburg benthic chamber landers: Applications and quality control. *Journal of Marine*
960 *Systems*, *214*, 103475. https://doi.org/10.1016/j.jmarsys.2020.103475
961 Korup, O., Seidemann, J., & Mohr, C. H. (2019). Increased landslide activity on forested hillslopes following two
962 recent volcanic eruptions in Chile. *Nature Geoscience*, *12*(4), 284–289. https://doi.org/10.1038/s41561-
963 019-0315-9
964 Krajewska, M., Szymczak-Żyła, M., Tylmann, W., & Kowalewska, G. (2020). Climate change impact on primary
965 production and phytoplankton taxonomy in Western Spitsbergen fjords based on pigments in sediments.
966 *Global and Planetary Change*, *189*, 103158. https://doi.org/10.1016/j.gloplacha.2020.103158

967 Kristensen, E., Ahmed, S. I., & Devol, A. H. (1995). Aerobic and anaerobic decomposition of organic matter in
968 marine sediment: Which is fastest? *Limnology and Oceanography*, *40*(8), 1430–1437.
969 https://doi.org/10.4319/lo.1995.40.8.1430
970 Kuliński, K., Kędra, M., Legeżyńska, J., Gluchowska, M., & Zaborska, A. (2014). Particulate organic matter sinks
971 and sources in high Arctic fjord. *Journal of Marine Systems*, *139*, 27–37.
972 https://doi.org/10.1016/j.jmarsys.2014.04.018
973 Kwon, S., & Pignatello, J. J. (2005). Effect of Natural Organic Substances on the Surface and Adsorptive Properties
974 of Environmental Black Carbon (Char): Pseudo Pore Blockage by Model Lipid Components and Its
975 Implications for N_2-Probed Surface Properties of Natural Sorbents. *Environmental Science & Technology*,
976 *39*(20), 7932–7939. https://doi.org/10.1021/es050976h
977 Lafon, A., Silva, N., & Vargas, C. A. (2014). Contribution of allochthonous organic carbon across the Serrano River
978 Basin and the adjacent fjord system in Southern Chilean Patagonia: Insights from the combined use of
979 stable isotope and fatty acid biomarkers. *Progress in Oceanography*, *129*, 98–113.
980 https://doi.org/10.1016/j.pocean.2014.03.004
981 Lindahl, O, & Hernroth, L. (1988). Large-scale and long-term variations in the zooplankton community of the
982 Gullmar fjord, Sweden, in relation to advective processes. *Marine Ecology Progress Series*, *43*, 161–171.
983 https://doi.org/10.3354/meps043161
984 Lindahl, Odd, Anderson, L., & Belgrano, A. (2009). Primary phytoplankton productivity in the Gullmar Fjord,
985 Sweden: Am evaluation of the 1985-1008 time series. Swedish Environmental Protection Agency.
986 Lindroth, Peter., & Mopper, Kenneth. (1979). High performance liquid chromatographic determination of
987 subpicomole amounts of amino acids by precolumn fluorescence derivatization with o-phthaldialdehyde.
988 *Analytical Chemistry*, *51*(11), 1667–1674. https://doi.org/10.1021/ac50047a019
989 Loh, P. S., Miller, A. E. J., Reeves, A. D., Harvey, S. M., & Overnell, J. (2008). Optimised recovery of lignin-
990 derived phenols in a Scottish fjord by the CuO oxidation method. *Journal of Environmental Monitoring*,
991 *10*(10), 1187. https://doi.org/10.1039/b808970a
992 Louchouarn, P., Lucotte, M., Canuel, R., Gagné, J.-P., & Richard, L.-F. (1997). Sources and early diagenesis of
993 lignin and bulk organic matter in the sediments of the Lower St. Lawrence Estuary and the Saguenay Fjord.
994 *Marine Chemistry*, *58*(1–2), 3–26. https://doi.org/10.1016/S0304-4203(97)00022-4

995 Louchouarn, P., Amon, R. M. W., Duan, S., Pondell, C., Seward, S. M., & White, N. (2010). Analysis of lignin-
996 derived phenols in standard reference materials and ocean dissolved organic matter by gas
997 chromatography/tandem mass spectrometry. *Marine Chemistry*, *118*(1–2), 85–97.
998 https://doi.org/10.1016/j.marchem.2009.11.003
999 Mai-Thi, N.-N., St-Onge, G., & Tremblay, L. (2017). Contrasting fates of organic matter in locations having
1000 different organic matter inputs and bottom water O 2 concentrations. *Estuarine, Coastal and Shelf Science*,
1001 *198*, 63–72. https://doi.org/10.1016/j.ecss.2017.08.044
1002 Mauring, A., & Gäfvert, T. (2013). Radon tightness of different sample sealing methods for gamma spectrometric
1003 measurements of 226Ra. *Applied Radiation and Isotopes*, *81*, 92–95.
1004 https://doi.org/10.1016/j.apradiso.2013.03.022
1005 McQuoid, M. R., & Nordberg, K. (2003). The diatom Paralia sulcata as an environmental indicator species in
1006 coastal sediments. *Estuarine, Coastal and Shelf Science*, *56*(2), 339–354. https://doi.org/10.1016/S0272-
1007 7714(02)00187-7
1008 Menzel, P., Gaye, B., Wiesner, M. G., Prasad, S., Stebich, M., Das, B. K., et al. (2013). Influence of bottom water
1009 anoxia on nitrogen isotopic ratios and amino acid contributions of recent sediments from small eutrophic
1010 Lonar Lake, central India. *Limnology and Oceanography*, *58*(3), 1061–1074.
1011 https://doi.org/10.4319/lo.2013.58.3.1061
1012 Menzel, P., Anupama, K., Basavaiah, N., Das, B. K., Gaye, B., Herrmann, N., & Prasad, S. (2015). The use of
1013 amino acid analyses in (palaeo-) limnological investigations: A comparative study of four Indian lakes in
1014 different climate regimes. *Geochimica et Cosmochimica Acta*, *160*, 25–37.
1015 https://doi.org/10.1016/j.gca.2015.03.028
1016 Middelburg, J., & Levin, L. (2009). Coastal hypoxia and sediment biogeochemistry. *Biogeosciences*, *6*(7), 1273–
1017 1293.
1018 Middelburg, J. J. (2018). Reviews and syntheses: to the bottom of carbon processing at the seafloor. *Biogeosciences*,
1019 *15*(2), 413–427. https://doi.org/10.5194/bg-15-413-2018
1020 Nuwer, J. M., & Keil, R. G. (2005). Sedimentary organic matter geochemistry of Clayoquot Sound, Vancouver
1021 Island, British Columbia. *Limnology and Oceanography*, *50*(4), 1119–1128.
1022 https://doi.org/10.4319/lo.2005.50.4.1119

1023 Olofsson, M., Robertson, E. K., Edler, L., Arneborg, L., Whitehouse, M. J., & Ploug, H. (2019). Nitrate and
1024 ammonium fluxes to diatoms and dinoflagellates at a single cell level in mixed field communities in the
1025 sea. *Scientific Reports*, *9*(1), 1424. https://doi.org/10.1038/s41598-018-38059-4
1026 Opsahl, S., & Benner, R. (1995). Early diagenesis of vascular plant tissues: Lignin and cutin decomposition and
1027 biogeochemical implications. *Geochimica et Cosmochimica Acta*, *59*(23), 4889–4904.
1028 https://doi.org/10.1016/0016-7037(95)00348-7
1029 Otto, A., & Simpson, M. J. (2006). Evaluation of CuO oxidation parameters for determining the source and stage of
1030 lignin degradation in soil. *Biogeochemistry*, *80*(2), 121–142. https://doi.org/10.1007/s10533-006-9014-x
1031 Polovodova Asteman, I., & Nordberg, K. (2013). Foraminiferal fauna from a deep basin in Gullmar Fjord: The
1032 influence of seasonal hypoxia and North Atlantic Oscillation. *Journal of Sea Research*, *79*, 40–49.
1033 https://doi.org/10.1016/j.seares.2013.02.001
1034 Polovodova, I., Nordberg, K., & Filipsson, H. L. (2011). The benthic foraminiferal record of the Medieval Warm
1035 Period and the recent warming in the Gullmar Fjord, Swedish west coast. *Marine Micropaleontology*,
1036 *81*(3–4), 95–106. https://doi.org/10.1016/j.marmicro.2011.09.002
1037 Prahl, F. G., Ertel, J. R., Goni, M. A., Sparrow, M. A., & Eversmeyer, B. (1994). Terrestrial organic carbon
1038 contributions to sediments on the Washington margin. *Geochimica et Cosmochimica Acta*, *58*(14), 3035–
1039 3048. https://doi.org/10.1016/0016-7037(94)90177-5
1040 Ramirez, M. T., Allison, M. A., Bianchi, T. S., Cui, X., Savage, C., Schüller, S. E., et al. (2016). Modern deposition
1041 rates and patterns of organic carbon burial in Fiordland, New Zealand. *Geophysical Research Letters*,
1042 *43*(22). https://doi.org/10.1002/2016GL070021
1043 Reuss, N., Conley, D. J., & Bianchi, T. S. (2005). Preservation conditions and the use of sediment pigments as a tool
1044 for recent ecological reconstruction in four Northern European estuaries. *Marine Chemistry*, *95*(3–4), 283–
1045 302. https://doi.org/10.1016/j.marchem.2004.10.002
1046 Roy, S., Llewellyn, C. A., Skarstad Egeland, E., & Johnsen. (2011). *Phytoplankton pigments: characterization,*
1047 *chemotaxonomy and applications in oceanography*. Cambridge (GB): Cambridge university press.
1048 Ruben, M., Hefter, J., Schubotz, F., Geibert, W., Butzin, M., Gentz, T., et al. (2023). Fossil organic carbon
1049 utilization in marine Arctic fjord sediments by subsurface micro-organisms. *Nature Geoscience*, *16*(7),
1050 625–630. https://doi.org/10.1038/s41561-023-01198-z

1051 Sadeghi, M., Morris, G. A., Carranza, E. J. M., Ladenberger, A., & Andersson, M. (2013). Rare earth element
1052 distribution and mineralization in Sweden: An application of principal component analysis to FOREGS soil
1053 geochemistry. *Journal of Geochemical Exploration*, *133*, 160–175.
1054 https://doi.org/10.1016/j.gexplo.2012.10.015
1055 Sampere, T. P., Bianchi, T. S., Wakeham, S. G., & Allison, M. A. (2008). Sources of organic matter in surface
1056 sediments of the Louisiana Continental margin: Effects of major depositional/transport pathways and
1057 Hurricane Ivan. *Continental Shelf Research*, *28*(17), 2472–2487. https://doi.org/10.1016/j.csr.2008.06.009
1058 Schlitzer, & Reiner. (2023). Ocean Data View. Retrieved from https://odv.awi.de
1059 Schüller, S., & Savage, C. (2011). Spatial distribution of diatom and pigment sedimentary records in surface
1060 sediments in Doubtful Sound, Fiordland, New Zealand. *New Zealand Journal of Marine and Freshwater*
1061 *Research*, *45*(4), 591–608. https://doi.org/10.1080/00288330.2011.561865
1062 Schüller, S. E., Allison, M. A., Bianchi, T. S., Tian, F., & Savage, C. (2013). Historical variability in past
1063 phytoplankton abundance and composition in Doubtful Sound, New Zealand. *Continental Shelf Research*,
1064 *69*, 110–122. https://doi.org/10.1016/j.csr.2013.09.021
1065 Sepúlveda, J., Pantoja, S., & Hughen, K. A. (2011). Sources and distribution of organic matter in northern Patagonia
1066 fjords, Chile (~44–47°S): A multi-tracer approach for carbon cycling assessment. *Continental Shelf*
1067 *Research*, *31*(3–4), 315–329. https://doi.org/10.1016/j.csr.2010.05.013
1068 Shields, M. R., Bianchi, T. S., Kolker, A. S., Kenney, W. F., Mohrig, D., Osborne, T. Z., & Curtis, J. H. (2019).
1069 Factors Controlling Storage, Sources, and Diagenetic State of Organic Carbon in a Prograding Subaerial
1070 Delta: Wax Lake Delta, Louisiana. *Journal of Geophysical Research: Biogeosciences*, *124*(5), 1115–1131.
1071 https://doi.org/10.1029/2018JG004683
1072 Shields, M. R., Bianchi, T. S., Osburn, C. L., Kinsey, J. D., Ziervogel, K., Schnetzer, A., & Corradino, G. (2019).
1073 Linking chromophoric organic matter transformation with biomarker indices in a marine phytoplankton
1074 growth and degradation experiment. *Marine Chemistry*, *214*, 103665.
1075 https://doi.org/10.1016/j.marchem.2019.103665
1076 Siegenthaler, U., & Sarmiento, J. L. (1993). Atmospheric carbon dioxide and the ocean. *Nature*, *365*(6442), 119–
1077 125. https://doi.org/10.1038/365119a0

1078 Silva, N., & Vargas, C. A. (2014). Hypoxia in Chilean Patagonian Fjords. *Progress in Oceanography*, *129*, 62–74.
1079 https://doi.org/10.1016/j.pocean.2014.05.016
1080 Smeaton, C., & Austin, W. E. N. (2022). Understanding the Role of Terrestrial and Marine Carbon in the Mid-
1081 Latitude Fjords of Scotland. *Global Biogeochemical Cycles*, *36*(11), e2022GB007434.
1082 https://doi.org/10.1029/2022GB007434
1083 Smeaton, Craig, Yang, H., & Austin, W. E. N. (2021). Carbon burial in the mid-latitude fjords of Scotland. *Marine*
1084 *Geology*, *441*, 106618. https://doi.org/10.1016/j.margeo.2021.106618
1085 SMHI. (2023). SharkWeb [Data set]. Swedish Meteorological and Hydrological Institute (SMHI). Retrieved from
1086 https://sharkweb.smhi.se/
1087 Smith, R. W., Bianchi, T. S., & Savage, C. (2010). Comparison of lignin phenols and branched/isoprenoid
1088 tetraethers (BIT index) as indices of terrestrial organic matter in Doubtful Sound, Fiordland, New Zealand.
1089 *Organic Geochemistry*, *41*(3), 281–290. https://doi.org/10.1016/j.orggeochem.2009.10.009
1090 Smith, R. W., Bianchi, T. S., Allison, M., Savage, C., & Galy, V. (2015). High rates of organic carbon burial in fjord
1091 sediments globally. *Nature Geoscience*, *8*(6), 450–453.
1092 Smittenberg, R. H., Pancost, R. D., Hopmans, E. C., Paetzel, M., & Sinninghe Damsté, J. S. (2004). A 400-year
1093 record of environmental change in an euxinic fjord as revealed by the sedimentary biomarker record.
1094 *Palaeogeography, Palaeoclimatology, Palaeoecology*, *202*(3–4), 331–351. https://doi.org/10.1016/S0031-
1095 0182(03)00642-4
1096 Statistics Sweden. (2023). Land use in Sweden 2020 [Data set]. Official Statistics of Sweden. Retrieved from
1097 https://www.statistikdatabasen.scb.se/pxweb/en/ssd/START__MI__MI0803__MI0803A/MarkanvN/table/t
1098 ableViewLayout1/
1099 Stigebrandt, A., Liljebladh, B., de Brabandere, L., Forth, M., Granmo, Å., Hall, P., et al. (2015). An Experiment
1100 with Forced Oxygenation of the Deepwater of the Anoxic By Fjord, Western Sweden. *AMBIO*, *44*(1), 42–
1101 54. https://doi.org/10.1007/s13280-014-0524-9
1102 Stock, B. C., Jackson, A. L., Ward, E. J., Parnell, A. C., Phillips, D. L., & Semmens, B. X. (2018). Analyzing
1103 mixing systems using a new generation of Bayesian tracer mixing models. *PeerJ*, *6*, e5096.
1104 https://doi.org/10.7717/peerj.5096

1105 Stroeven, A. P., Hättestrand, C., Kleman, J., Heyman, J., Fabel, D., Fredin, O., et al. (2016). Deglaciation of
1106 Fennoscandia. *Quaternary Science Reviews*, *147*, 91–121. https://doi.org/10.1016/j.quascirev.2015.09.016
1107 Sun, M.-Y., Lee, C., & Aller, R. C. (1993). Anoxic and oxic degradation of ^{14}C-labeled chloropigments and a ^{14}C-
1108 labeled diatom in Long Island Sound sediments. *Limnology and Oceanography*, *38*(7), 1438–1451.
1109 https://doi.org/10.4319/lo.1993.38.7.1438
1110 Svansson, A. (1984). *Hydrography of the Gullmar Fjord: (Gullmarsfjordens Hydrografi)*. Hydrografiska
1111 laboratoriet.
1112 Szymczak-Żyła, M., Krajewska, M., Winogradow, A., Zaborska, A., Breedveld, G. D., & Kowalewska, G. (2017).
1113 Tracking trends in eutrophication based on pigments in recent coastal sediments. *Oceanologia*, *59*(1), 1–17.
1114 https://doi.org/10.1016/j.oceano.2016.08.003
1115 Tiselius, P, Hansen, B., & Calliari, D. (2012). Fatty acid transformation in zooplankton: from seston to benthos.
1116 *Marine Ecology Progress Series*, *446*, 131–144. https://doi.org/10.3354/meps09479
1117 Tiselius, Peter, & Kuylenstierna, M. (1996). Growth and decline of a diatom spring bloom phytoplankton species
1118 composition, formation of marine snow and the role of heterotrophic dinoflagellates. *Journal of Plankton*
1119 *Research*, *18*(2), 133–155. https://doi.org/10.1093/plankt/18.2.133
1120 Tiselius, Peter, Belgrano, A., Andersson, L., & Lindahl, O. (2016). Primary productivity in a coastal ecosystem: a
1121 trophic perspective on a long-term time series. *Journal of Plankton Research*, *38*(4), 1092–1102.
1122 https://doi.org/10.1093/plankt/fbv094
1123 Törnquist, P., Eriksson, M., Olszewski, G., Carlsson, M., López-Lora, M., & Pettersson, H. B. L. (2023). On the use
1124 of dated sediments to investigate historical nuclear discharges. *Marine Pollution Bulletin*, *188*, 114637.
1125 https://doi.org/10.1016/j.marpolbul.2023.114637
1126 Van De Velde, S. J., Hylén, A., Eriksson, M., James, R. K., Kononets, M. Y., Robertson, E. K., & Hall, P. O. J.
1127 (2023). Exceptionally high respiration rates in the reactive surface layer of sediments underlying oxygen-
1128 deficient bottom waters. *Proceedings of the Royal Society A: Mathematical, Physical and Engineering*
1129 *Sciences*, *479*(2275), 20230189. https://doi.org/10.1098/rspa.2023.0189
1130 Van Nugteren, P., Moodley, L., Brummer, G.-J., Heip, C. H. R., Herman, P. M. J., & Middelburg, J. J. (2009).
1131 Seafloor ecosystem functioning: the importance of organic matter priming. *Marine Biology*, *156*(11), 2277–
1132 2287. https://doi.org/10.1007/s00227-009-1255-5

1133 Vandewiele, S., Cowie, G., Soetaert, K., & Middelburg, J. J. (2009). Amino acid biogeochemistry and organic
1134 matter degradation state across the Pakistan margin oxygen minimum zone. *Deep Sea Research Part II:*
1135 *Topical Studies in Oceanography*, *56*(6–7), 376–392. https://doi.org/10.1016/j.dsr2.2008.05.035
1136 Vargas, C., Tönnesson, K., Sell, A., Maar, M., Møller, E., Zervoudaki, T., et al. (2002). Importance of copepods
1137 versus appendicularians in vertical carbon fluxes in a Swedish fjord. *Marine Ecology Progress Series*, *241*,
1138 125–138. https://doi.org/10.3354/meps241125
1139 Viktorsson, L., Kononets, M., Roos, P., & Hall, P. O. J. (2013). Recycling and burial of phosphorus in sediments of
1140 an anoxic fjord—the By Fjord, western Sweden. *Journal of Marine Research*, *71*(5), 351–374.
1141 https://doi.org/10.1357/002224013810921636
1142 Waite, A. M., Gustafsson, Ö., Lindahl, O., & Tiselius, P. (2005). Linking ecosystem dynamics and biogeochemistry:
1143 Sinking fractionation of organic carbon in a Swedish fjord. *Limnology and Oceanography*, *50*(2), 658–671.
1144 https://doi.org/10.4319/lo.2005.50.2.0658
1145 Wakeham, S. G., Lee, C., Hedges, J. I., Hernes, P. J., & Peterson, M. J. (1997). Molecular indicators of diagenetic
1146 status in marine organic matter. *Geochimica et Cosmochimica Acta*, *61*(24), 5363–5369.
1147 https://doi.org/10.1016/S0016-7037(97)00312-8
1148 Walsh, E. M., Ingalls, A. E., & Keil, R. G. (2008). Sources and transport of terrestrial organic matter in Vancouver
1149 Island fjords and the Vancouver-Washington Margin: A multiproxy approach using d13Corg, lignin
1150 phenols, and the ether lipid BIT index. *Limnology and Oceanography*, *53*(3), 1054–1063.
1151 https://doi.org/10.4319/lo.2008.53.3.1054
1152 Wang, K., Chen, J., Jin, H., Li, H., & Zhang, W. (2018). Organic matter degradation in surface sediments of the
1153 Changjiang estuary: Evidence from amino acids. *Science of The Total Environment*, *637–638*, 1004–1013.
1154 https://doi.org/10.1016/j.scitotenv.2018.04.242
1155 Włodarska-Kowalczuk, M., Mazurkiewicz, M., Górska, B., Michel, L. N., Jankowska, E., & Zaborska, A. (2019).
1156 Organic carbon origin, benthic faunal consumption, and burial in sediments of Northern Atlantic and Arctic
1157 fjords (60–81°N). *Journal of Geophysical Research: Biogeosciences*, *124*(12), 3737–3751.
1158 https://doi.org/10.1029/2019JG005140
1159 Wright, S. W., & Jeffrey, S. W. (1997). High-resolution HPLC system for chlorophylls and carotenoids of marine
1160 phytoplankton. In S. W. Jeffrey, R. F. C. Mantoura, S. W. Wright, & International Council of Scientific

Unions (Eds.), *Phytoplankton pigments in oceanography: guidelines to modern methods* (pp. 327–360). Paris: UNESCO Pub.

Fjord, Station	Site ID	Water depth (m)	Bottom water DO (µM)	Long-term redox	SML depth (cm)	Surface mud content (<63 µm)	Surface OC:SA (mg OC m^{-2})	MAR (g m^{-2} yr^{-1})	OCAR (g m^{-2} yr^{-1})	$OC_{mar}AR$ (g m^{-2} yr^{-1})
By, Head	By-H	11	260	Oxic	0	91.6	1.1	470 ± 40	2 ± 1	1± 0.1
By, Center	By-C	46.5	0	Anoxic	0*	91.2	2.7	380 ± 10	12 ± 3	8 ± 2
By, Mouth	By-M	23	0	Anoxic	0*	95.4	2.4	840 ± 90	24 ± 3	18 ± 2
By AVG								**560 ± 50**	**13 ± 5**	**9 ± 4**
Gullmar, Head	Gullmar-H	26	175	Oxic	10	87.7	1.8	670 ± 80	16 ± 2	6 ± 1
Gullmar, Center	Gullmar-C	118	107	Seasonally Hypoxic	12	92.0	0.9	1500 ± 200	39 ± 5	32 ± 6
Gullmar, Mouth	Gullmar-M	57	164	Seasonally Hypoxic	4	93.1	1.4	2220 ± 220	57 ± 6	49 ± 5
Gullmar AVG								**1460 ± 100**	**38 ± 12**	**29 ± 10**
Hake, Head	Hake-H	21	213	Oxic	0	93.4	1.1	1150 ± 80	28 ± 2	26 ± 2
Hake, Center	Hake-C	32	199	Oxic	3	92.5	1.1	1640 ± 110	41 ± 3	37 ± 3
Hake, Mouth	Hake-M	41	204	Oxic	4	95.4	1.2	4700 ± 500	122 ± 14	107 ± 12
Hake AVG								**2500 ± 170**	**64 ± 20**	**56 ± 18**
Total AVG								**1500 ± 70**	**38 ± 24**	**31 ± 21**

Figure 1.

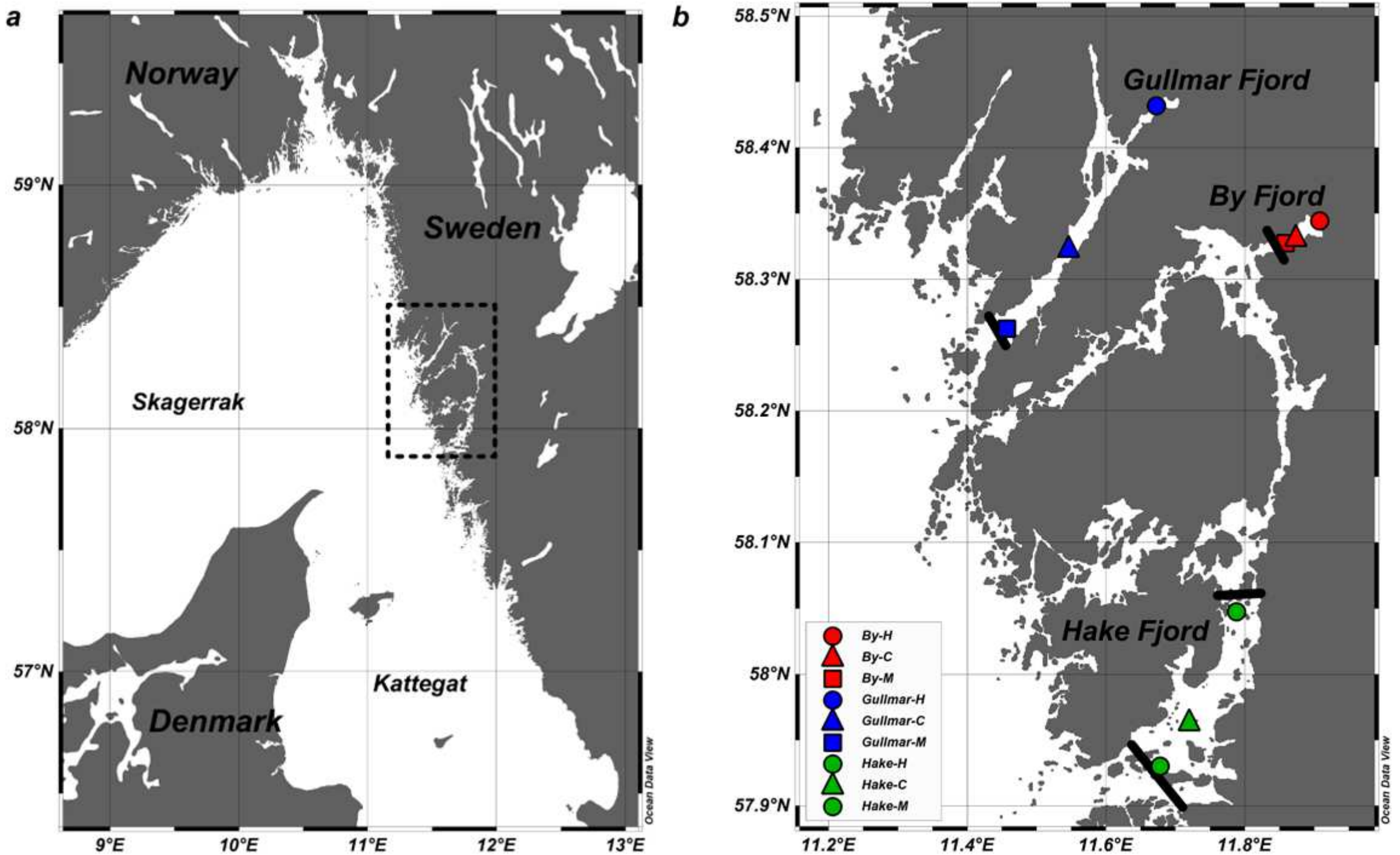
a
Norway
Sweden
Skagerrak
Kattegat
Denmark
59°N
58°N
57°N
9°E
10°E
11°E
12°E
13°E
Ocean Data View
b
Gullmar Fjord
By Fjord
Hake Fjord
58.5°N
58.4°N
58.3°N
58.2°N
58.1°N
58°N
57.9°N
11.2°E
11.4°E
11.6°E
11.8°E
By-H
By-C
By-M
Gullmar-H
Gullmar-C
Gullmar-M
Hake-H
Hake-C
Hake-M
Ocean Data View

Figure 2.

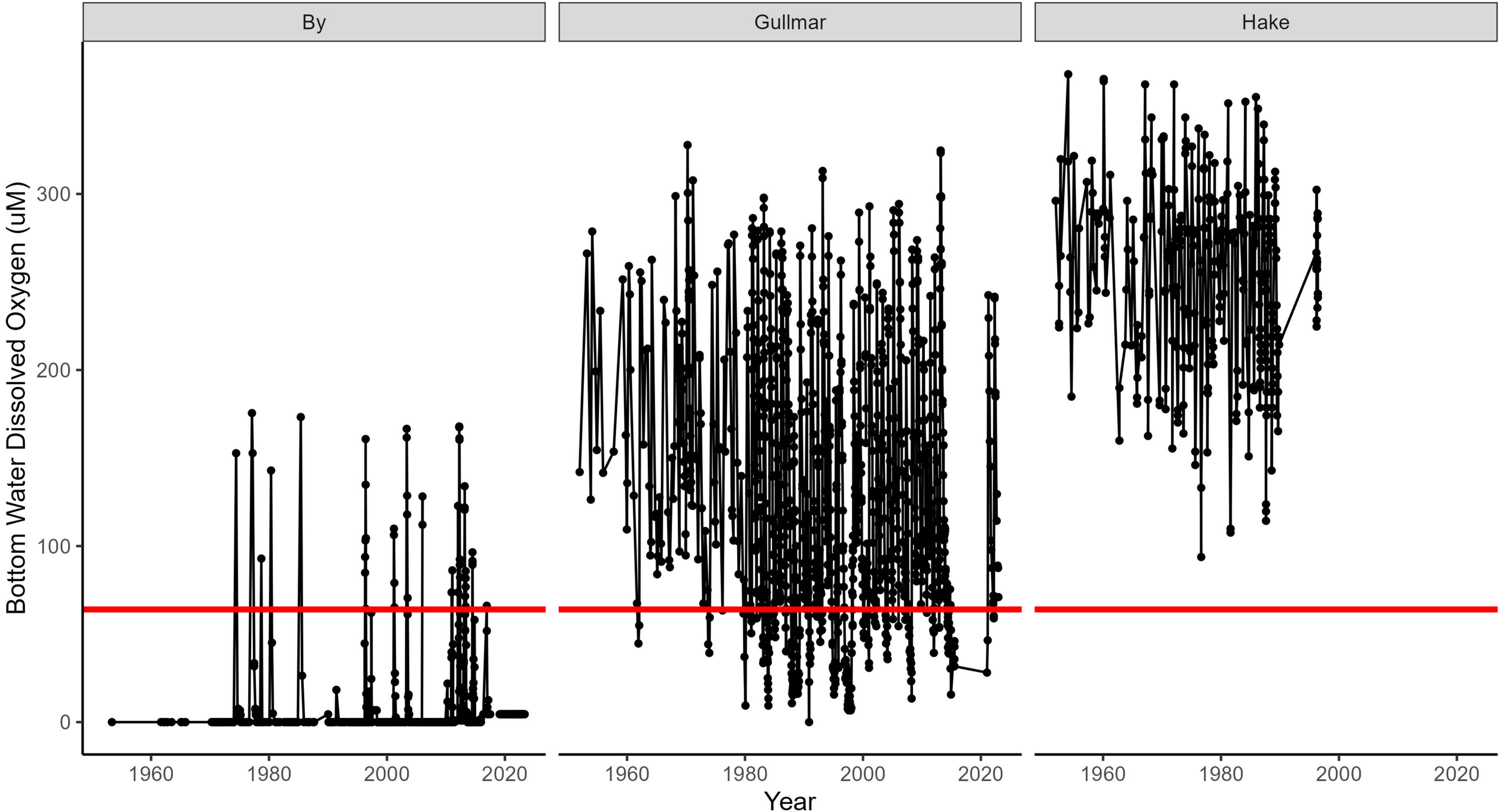
By
Gullmar
Hake
Bottom Water Dissolved Oxygen (uM)
300
200
100
0
1960
1980
2000
2020
Year

Figure 3.

a

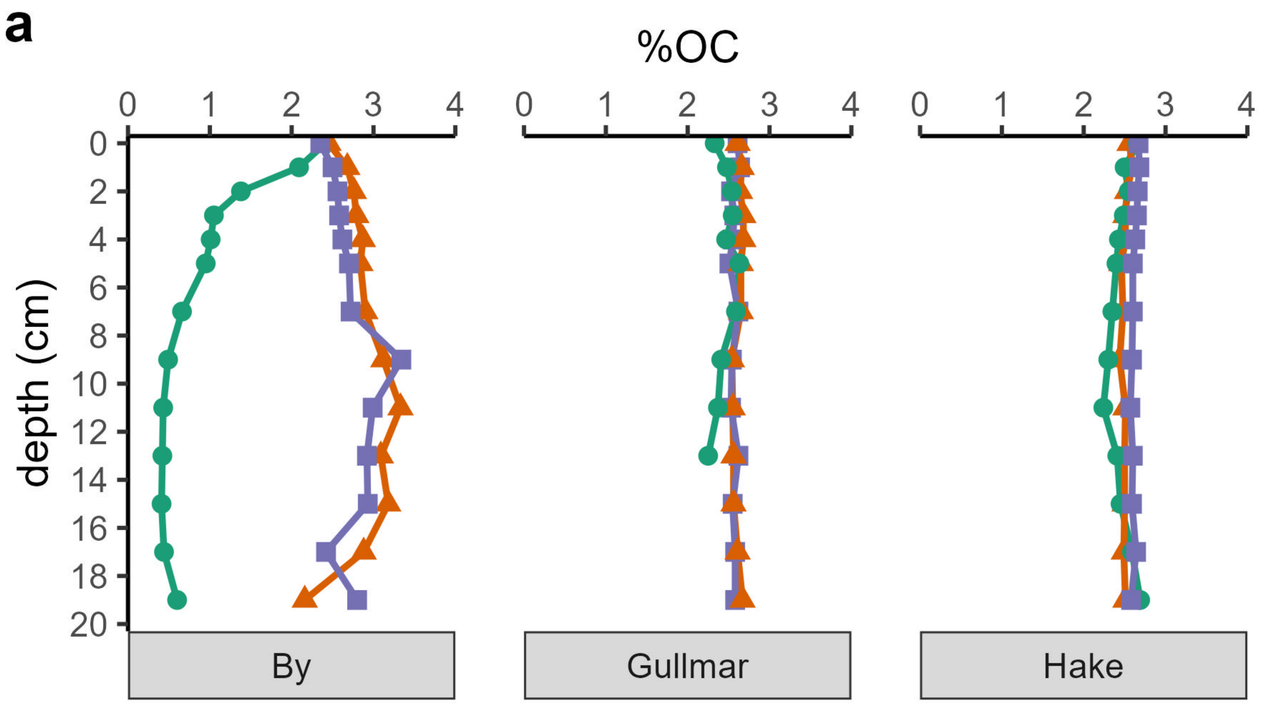

b

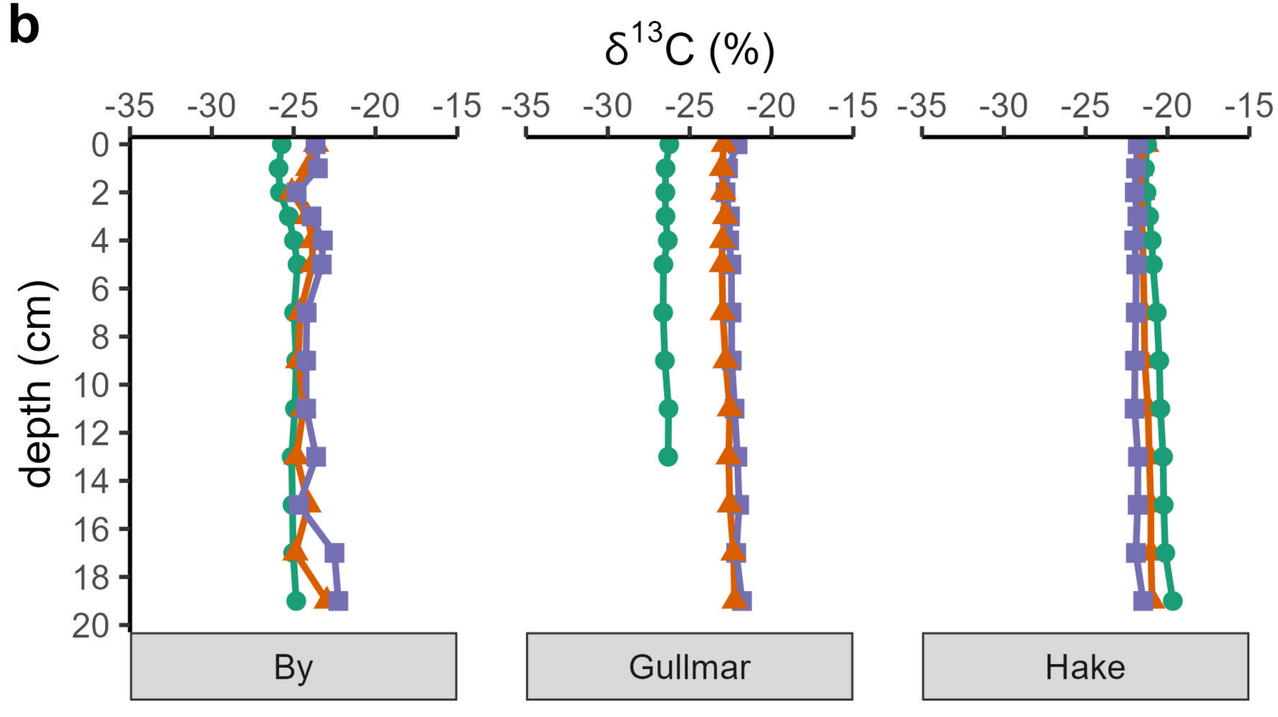

Site — head — center — mouth

c Surface Sediment Source

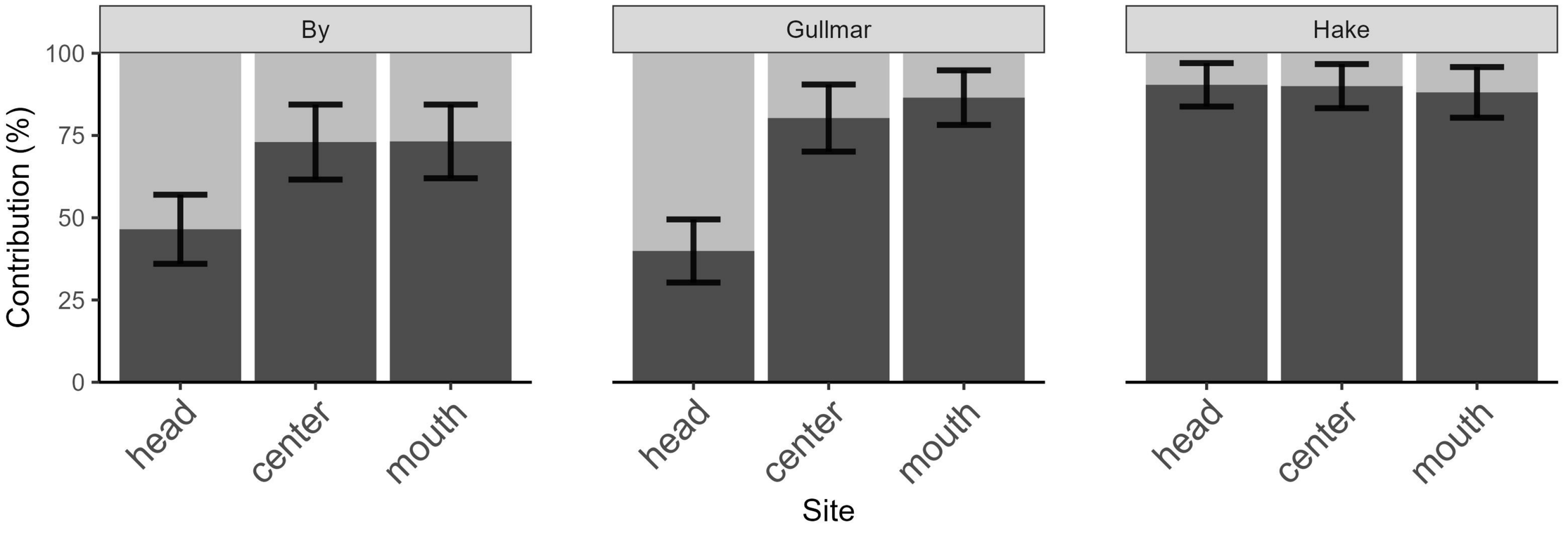

Figure 4.

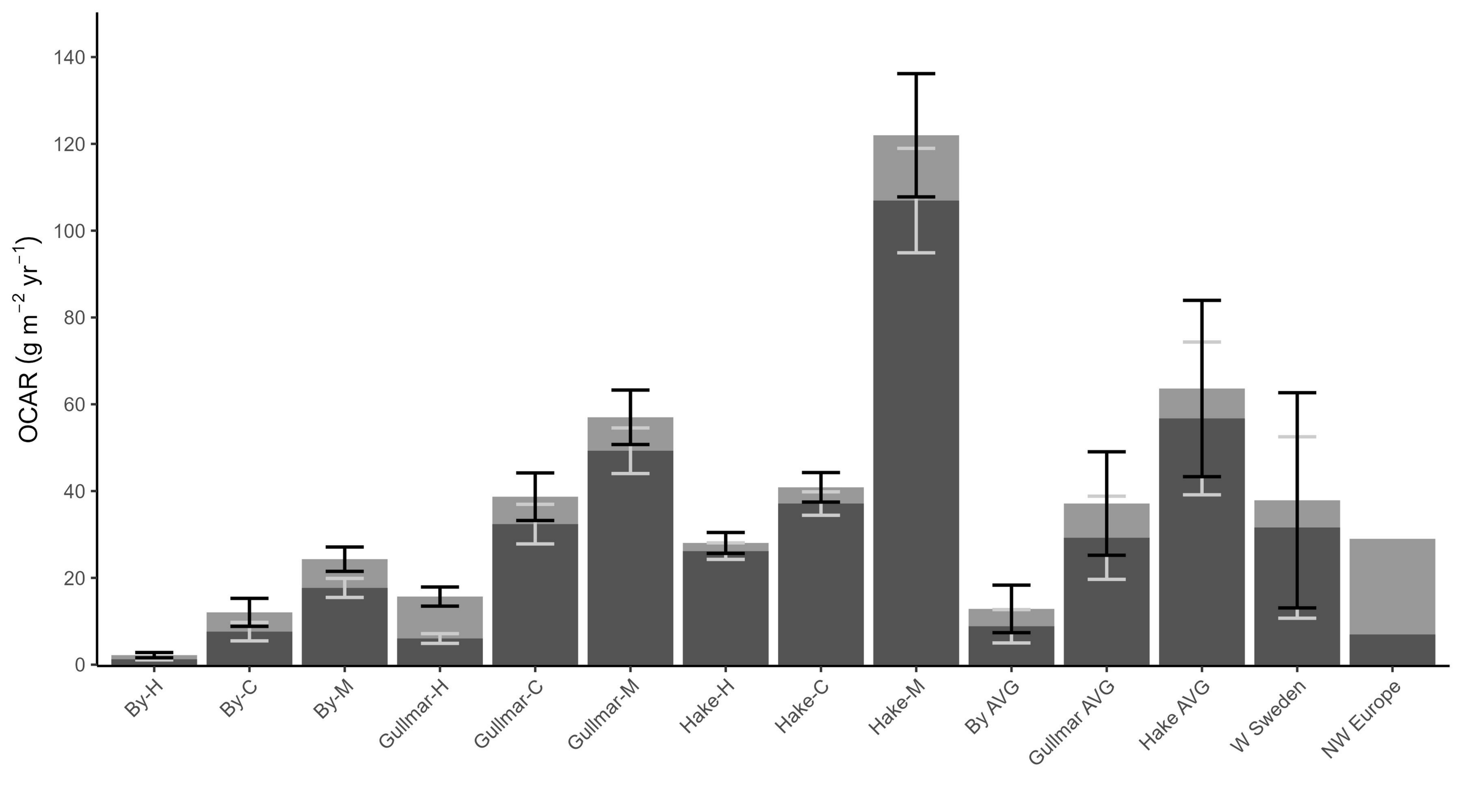
OCAR (g m^{-2} yr^{-1})
0
20
40
60
80
100
120
140
By-H
By-C
By-M
Gullmar-H
Gullmar-C
Gullmar-M
Hake-H
Hake-C
Hake-M
By AVG
Gullmar AVG
Hake AVG
W Sweden
NW Europe

Figure 5.

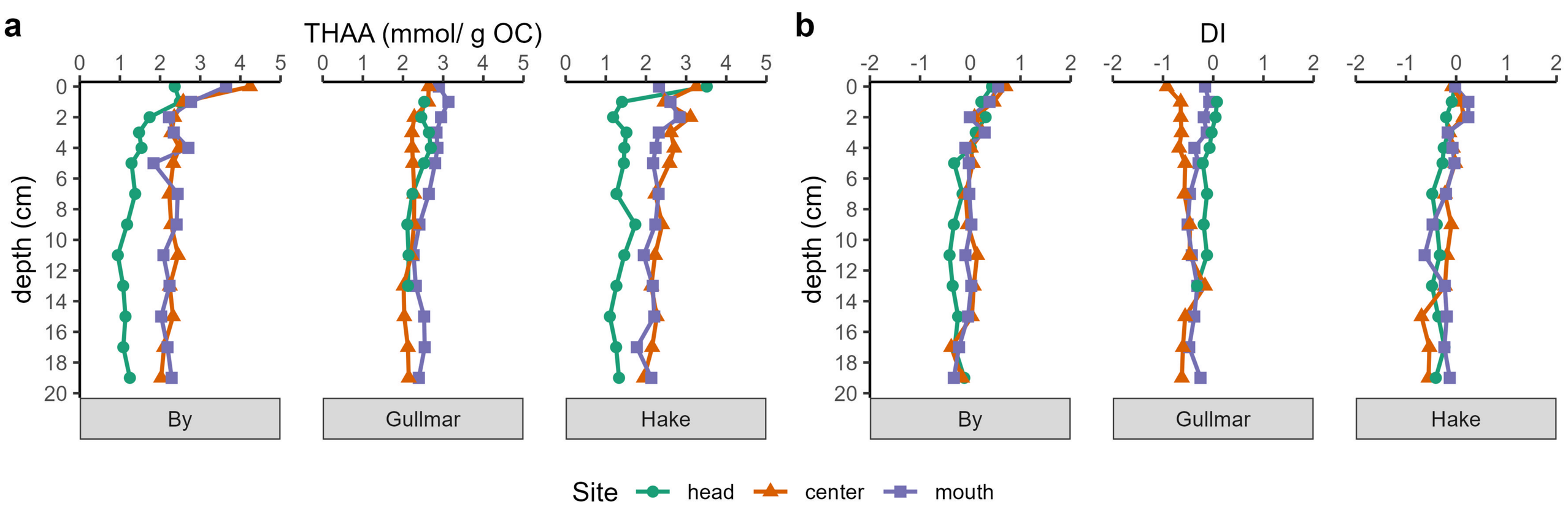
a
THAA (mmol/ g OC)
depth (cm)
By
Gullmar
Hake
b
DI
depth (cm)
By
Gullmar
Hake
Site
head
center
mouth

Figure 6.

a

Λ_8 (mg / 100 mg OC)

depth (cm)

By | Gullmar | Hake

b

$(acid/aldehyde)_v$

depth (cm)

By | Gullmar | Hake

c

By | Gullmar | Hake

S/V

C/V

A a G g

Site: head, center, mouth

Figure 7.

a
Chlorophyll-a (nmol / g OC)
b
Zeaxanthin (nmol / g OC)
c
Fucoxanthin (nmol / g OC)
d
Pheopigments (nmol / g OC)
e
Chl-a / Pheo
depth (cm)
By
Gullmar
Hake
Site
head
center
mouth

JGR: Biogeosciences

Supporting Information for

Burial of Organic Carbon in Swedish Fjord Sediments: Highlighting the Importance of Sediment Accumulation Rate in Relation to Fjord Redox Conditions

Emily G. Watts[1], Astrid Hylén[2], Per O.J. Hall[3], Mats Erikson[4], Elizabeth K. Robertson[3], William F. Kenney[5], and Thomas S. Bianchi[1]

[1]Department of Geological Sciences, University of Florida, Gainesville, USA
[2]Department of Biology, University of Antwerp, Wilrijk, Belgium
[3]Department of Marine Sciences, University of Gothenburg, Gothenburg, Sweden
[4]Department of Health, Medicine and Caring Sciences, Linkoping University, Linkoping Sweden
[5]Land Use and Environmental Change Institute, University of Florida, Gainesville, US

Contents of this file

Additional Supporting Information (Files uploaded separately)

Introduction

This study evaluates the role of organic carbon source and system redox conditions on organic carbon degradation and burial in fjord sediments. The supporting text provides more detailed information on the sample preparation for ^{210}Po measurement to use in ^{210}Pb age models (Text S1) and on the calculations of oxygen exposure times from sedimentary oxygen fluxes (Text S2). The supporting figures show excess ^{210}Pb profiles, C/N and δ^{15}N profiles, additional amino acid indices, individual amino acid mol percentages, and additional lignin indices (Figure S1 to Figure S5) downcore.

Text S1.

Additional ^{210}Pb Method Information:

- The sediment sample is weighed to about 0.5 g of dry weight and spiked with 0.1 Bq of ^{209}Po recovery standard
- The sample is digested in a mixture of nitric and hydrochloric acids using a microwave digestion system (CEM MARS 5 Microwave; Method 3051A). This step dissolves the sample and releases the polonium isotopes into the solution.
- The solution is filtered through a 1 µm membrane filter to remove any undissolved particles and transferred to a glass beaker. The solution is then evaporated to near dryness on a hot plate to reduce the volume.
- The residue is dissolved in a small amount of water and converted to chloride form by adding hydrochloric acid. The solution is then filtered through a 0.45 µm membrane filter to remove any insoluble complexes.
- The iron content of the solution is reduced by adding ascorbic acid, which converts Fe(III) to Fe(II). This prevents iron from depositing onto the silver disks and interfering with the polonium measurement.
- The silver disks are placed in the heated solution (80 °C) for 2 hours. Polonium isotopes are than spontaneously deposited onto the silver disks.
- The disks are then rinsed with water and ethanol and dried.
- The disks are measured between 1-3 days in an alpha spectrometry using 300 mm^2 PIPS detectors.

Text S2.

Oxygen penetration depths (OPDs) and oxygen exposure times (OETs) for center stations were calculated from bottom water oxygen concentrations at the time of sampling (Table 1) and sediment oxygen uptake rates. Sediment oxygen uptake rates, or benthic osygen fluxes, were measured as outlined in (Kononets et al., 2021). OPDs were calculated using the following equation from (Cai & Sayles, 1996):

$$L = 2\phi D_s \frac{[O_2]_{BW}}{F^0_{O_2}}$$

where L is OPD, ϕ is porosity, D_s is diffisivity of O_2 in the sediment, $[O_2]_{BW}$ is bottom water DO concentration, and F^0_{O2} is benthic oxygen flux. Sedimentary OET was calculated by dividing OPT by the linear sedimentation rate for each site.

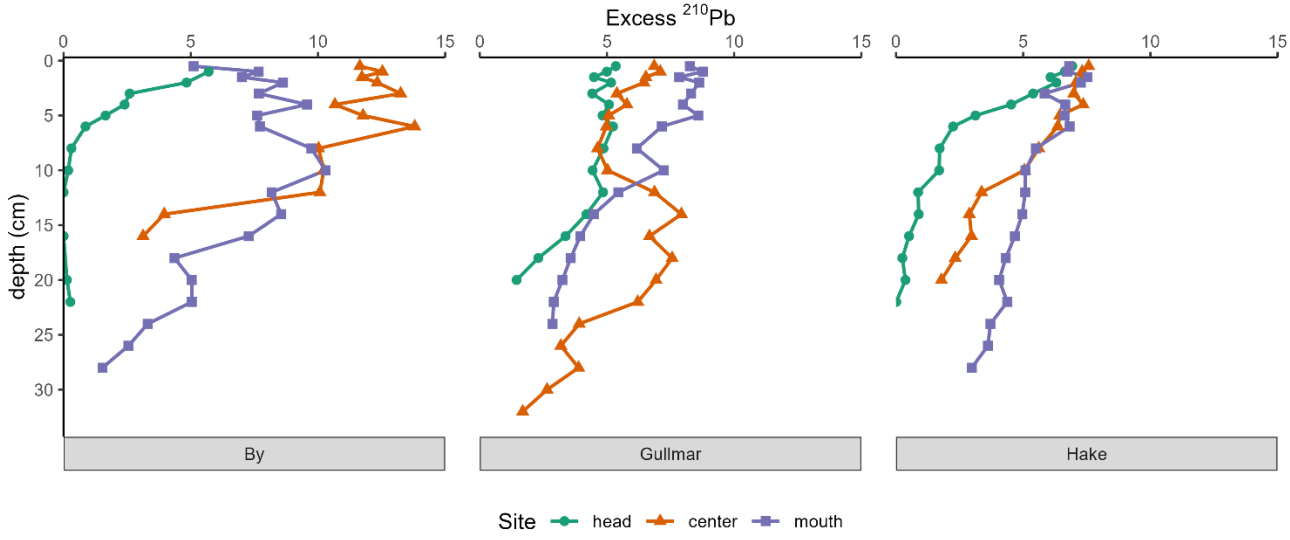

Figure S1. Downcore profiles of excess ^{210}Pb faceted by fjord id and color coordinated by site id.

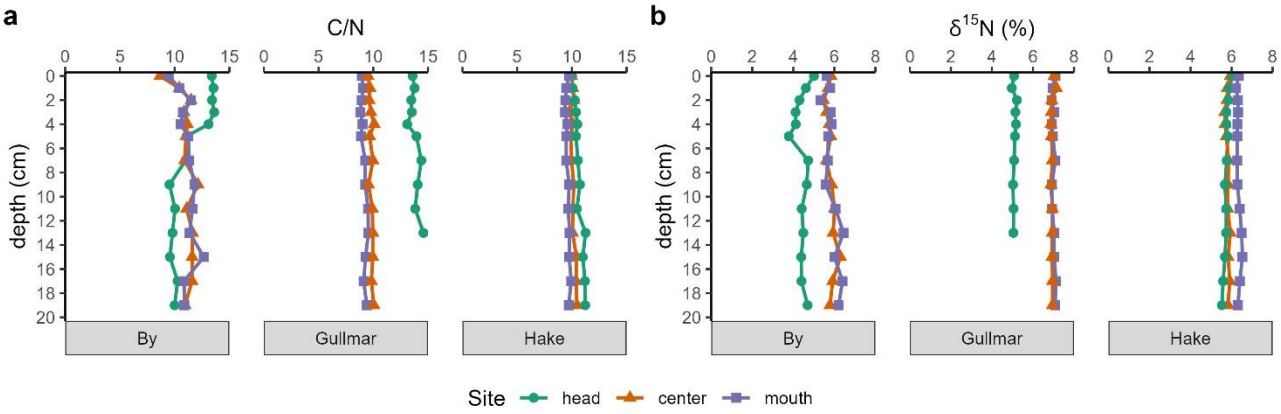

Fig. S2. Downcore profiles of a) C/N molar ratios and b) δ^{15}N (%) values. Each subfigure is faceted by fjord -id and color coordinated by site id.

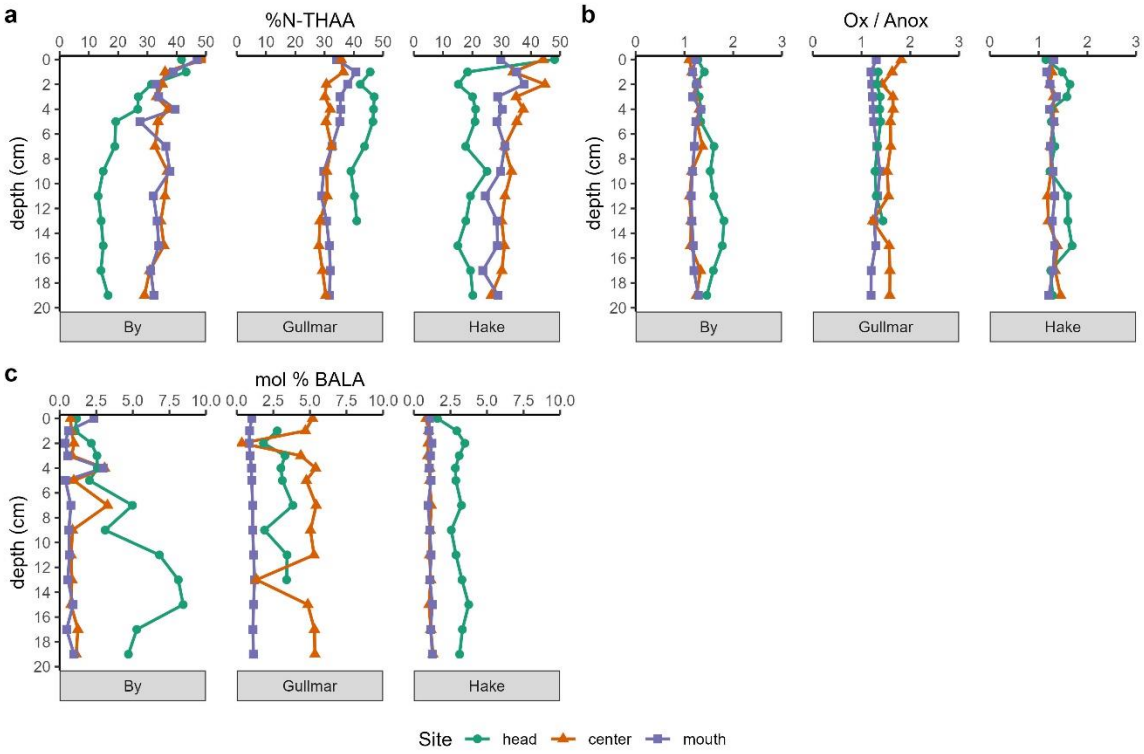

74

75 **Figure S3.** Downcore profiles of a) Portion of total nitrogen (TN) represented by total
76 hydrolyzable amino acids (THAA) nitrogen b) Ox/Anox ratios c) Mol percent β-alanine (BALA).
77 Each figure is faceted by fjord and color coordinated by site**.**

78

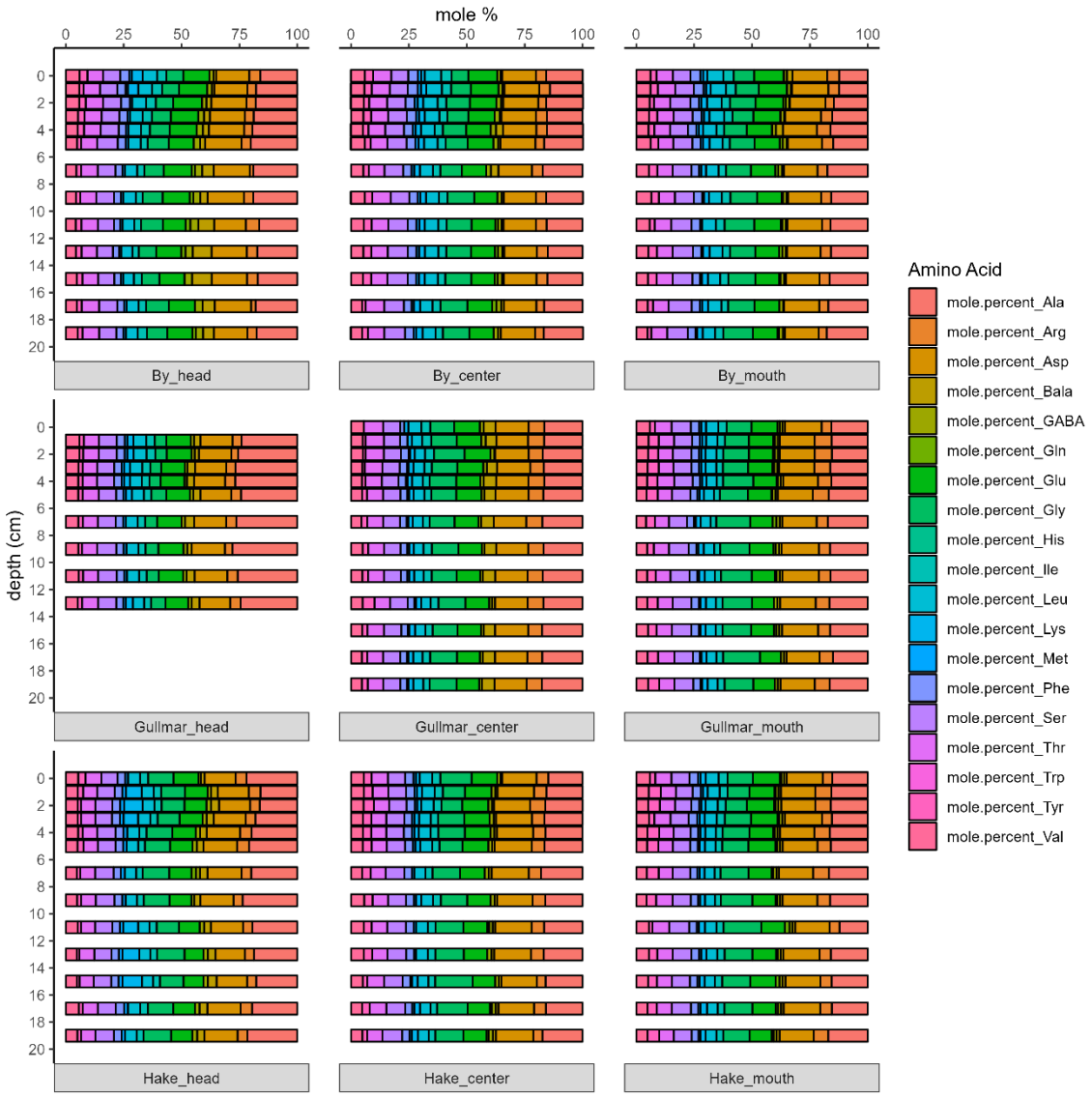

Fig. S4. Downcore profiles of mol % of amino acids by site.

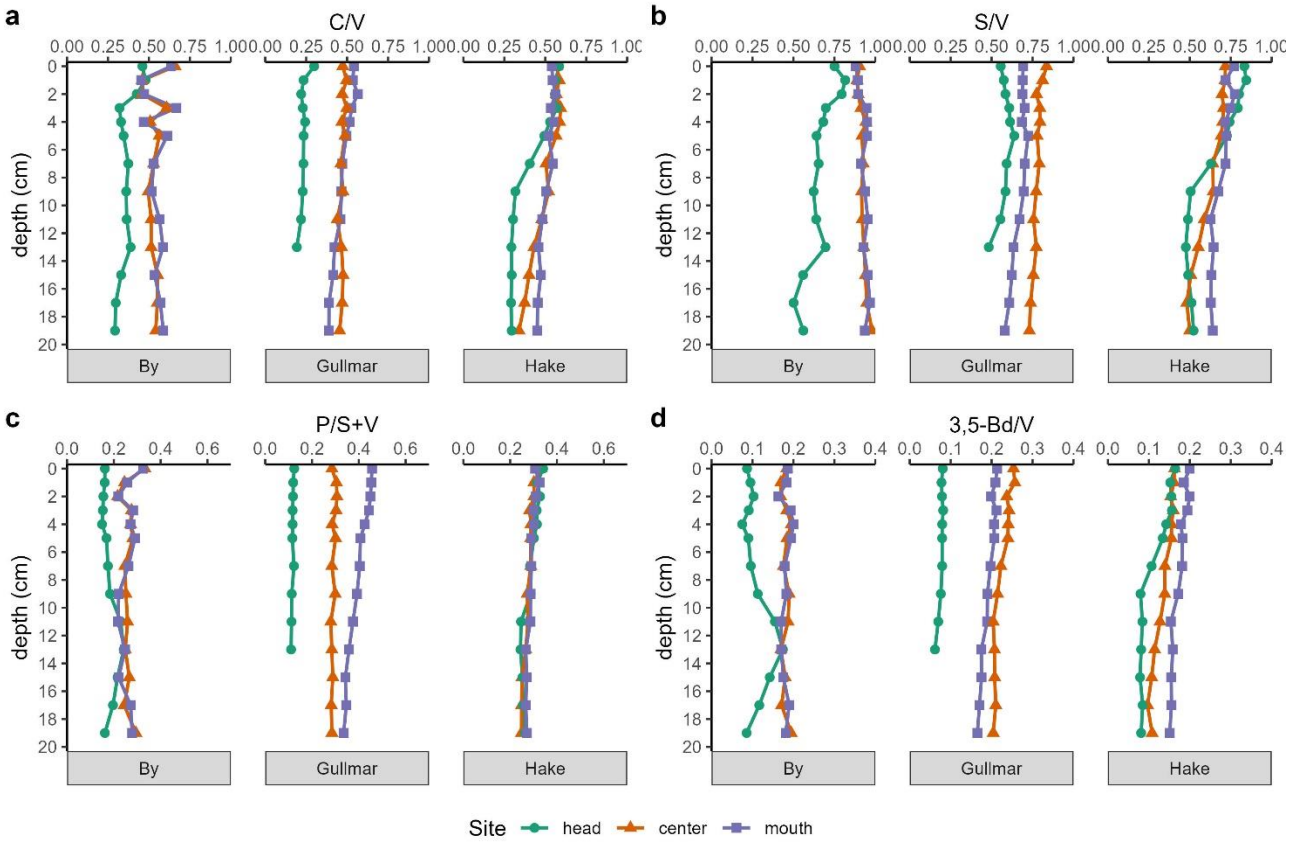

Fig. S5. Downcore profiles of a) Cinnamyl to vanillyl (C/V) ratios, b) Syringyl to vanillyl (S/V) ratios, c) p-hydroxy to cinnamyl + vanillyl (P/S+V) ratios, and d) 3-5-dibhydroxybenzoic acid (3,5-Bd) to vanillyl (3,5-Bd/V) ratios. Each subfigure is faceted by fjord id and color coded by site id.

Table S1. Summary data for bulk elemental data, amino acid data, lignin data, and pigment data. One standard deviation is reported with each mean.

Table S2. Bulk elemental data including %OC, $\delta^{13}C$, %N, $\delta^{15}N$, and C/N. The outputs from the Bayesian isotope mixing model are reported as fraction marine (Fmar), fraction terrestrial (Fterr), and the standard deviation (SD).

Table S3. Amino acid data including total hydrolyzable amino acid concentrations as μM (THAA_uM), normalized to g OC (THAA_umgc), normalized to g sediment (THAA_umgsed), and normalized to g nitrogen (THAA_umgn). Nitrogen-normalized yields (THAA.N.pct), DI score (DI_dauwe), and ox/anox ratios (thaa_redox) as well as mole percent for each amino acid are reported.

Table S4. Lignin data including Λ8 (lambda_8), total cinnamyl (c), syringyl (s), and vanillyl (v) phenols reported as mg (100 mg OC)$^{-1}$, (acid/aldehyde)$_v$ (adal.v), 3,5-dihydroxybenzoic acid to vanillyl ratios (bd.v), and C/V (c.v), S/V (s.v), and P/S+V (p.sv) ratios. Individual phenol concentrations are reported as mg (100 mg OC)$^{-1}$.

Table S5. Pigment concentrations of chlorophyll-a (chla), fucoxanthin (fuco), zeaxanthin (zea), and pheopigments (pheo) as nmol (g OC)$^{-1}$. Chlorophyll-a/pheopigment ratios are also reported

References

Cai, W. J., & Sayles, F. L. (1996). Oxygen penetration depths and fluxes in marine sediments. *Marine Chemistry*, *52*(2), 123–131. https://doi.org/10.1016/0304-4203(95)00081-X

Kononets, M., Tengberg, A., Nilsson, M., Ekeroth, N., Hylén, A., Robertson, E. K., et al. (2021). In situ incubations with the Gothenburg benthic chamber landers: Applications and quality control. *Journal of Marine Systems*, *214*, 103475. https://doi.org/10.1016/j.jmarsys.2020.103475